TiO_2, VO_2, and CrO_2: Electronic Structure and Role in C-H Bond Activation of Methane

by

Holden James Paz

A thesis submitted to the Graduate Faculty of
Auburn University
in partial fulfillment of the
requirements for the Degree of
Master of Chemistry

Auburn, Alabama
May 7, 2022

Keywords: transition metal dioxides, electronic structure, C-H bond activation

Approved by

Dr. Evangelos Miliordos, Chair, James E. Land Assistant Professor, Department of Chemistry and Biochemistry
Dr. Filip Pawłowski, Assistant Research Professor, Department of Chemistry and Biochemistry
Dr. Rashad Karimov, Assistant Professor, Department of Chemistry and Biochemistry

Abstract

Density functional theory and high-level ab initio electronic structure calculations are performed to study the titled transition metal dioxides and their ability to activate the C-H bond of methane. The electronic structure of the metal dioxides is elucidated to better inform later reactivity trends. The energy landscapes for the activation are constructed for different reaction pathways for all three metals. The effects of ammonia and chlorine ligands are considered both on individual metal dioxides and the reaction pathways.

Acknowledgments

I would first like to thank Dr. Evangelos Miliordos for his patience, guidance, help, and support through the past two years. In addition to him, I want to give a thank you to Dr. Filip Pawłowski for being not only a fantastic professor and academic powerhouse, but a good friend as well. As for Dr. Karimov, I would like to thank him for playing an important role in encouraging my connection to organic chemistry, for which I still have a soft spot. I want to thank Dr. Annie Gorden for the chance to collaborate and learn about the f-block elements, and Dr. Vince Ortiz both for kindling my interest in the mathematics that underpins quantum mechanics and for his personality that never failed to keep me engaged. I also want to thank Dr. Jason Upton for his support in beginning this step of my academic journey and taking my next.

I want to give a very special thanks to all of the students I had the pleasure of teaching in my organic lab sections. I cherished the time I had in lab with all of them, and that time is one of the things I will miss most in leaving this university. To all of my past students: I sincerely hope all of you get to live out your dreams.

Lastly, I would like to thank Alex. All of the little things she does every day make my life so much brighter, and I am excited to continue living life with her as my partner in crime.

Table of Contents

List of Tables

List of Figures

List of Abbreviations

ISR	Infinitely Separated Reactants
RIC	Reactant Interacting Complex
TS	Transition State
PIC	Product Interacting Complex
DFT	Density Functional Theory
CASPT2	Complete Active Space Second-order Perturbation Theory
MRCI	Multi-Reference Configuration Interaction Theory
MRCI+Q	Multi-Reference Configuration Interaction with Davidson Correction
CCSD(T)	Coupled-Cluster Singles and Doubles plus approximate Triples
C-(method)	e.g. C-MRCI - subset of core orbitals correlated

Chapter 1 : Introduction

Computational chemistry

Computational chemistry is a relatively young branch of chemistry in which chemical properties can be calculated with the use of computers. Since Moore's law has held, computational chemistry has grown in its capabilities and ability to give precise answers in shorter and shorter time frames. Computational chemistry is often used alongside experimental methods to give answers to geometric, energetic, and mechanistic questions about a molecular system at a significantly lower cost than that of laboratory experiments. Computational methods require electricity and, at the most, access to a supercomputer, a general-purpose machine that has use not only to a computational chemist, but to a range of professions. Laboratory experiments, on the other hand, can become prohibitively expensive while still only answering a limited number of questions about the system of interest, and the sometimes expensive raw materials are useful only to a small subset of researchers. With computational methods, exploration of a wider range of molecules is possible, including the space of molecules that may not have established and efficient synthetic maps to them. In recent years, acceptance of computational methods has become more mainstream, and their predictive power has been shown. The ability to run quantum mechanical calculations and interpret the results is now regarded as a useful tool in a chemist's toolbox.

Current methodologies in the computational chemistry space include, but are not limited to: molecular mechanics, *ab initio*, density functional theory, and molecular dynamics. The first of these methods relies on classical mechanics for its mathematical formalism, and the next two

are instead built on the Schrödinger equation. Molecular dynamics concerns the evolution of chemical systems in time, and can be applied to the first three. Although there is a significant increase in computational cost for the *ab initio* methods, they do provide more accurate results than other methods. The following thesis research consists of both *ab initio* multi-reference and density functional theory methodologies put to work on a series of transition metal dioxide systems with the goal of elucidating both their electronic structure and their ability to activate the C-H bond of methane.

Single-reference and multi-reference calculations

Hartree-Fock (HF) is the simplest *ab initio* method; the wavefunction is written as a determinant with entries corresponding to different spatial orbitals and spins of the electrons in those orbitals. This is a single-reference method, as only a single determinant is used to describe the system. For example, a two electron closed-shell system can be written as

$$2^{-0.5} \left(\psi_1(1)\alpha(1)\ \psi_1(2)\beta(2) - \psi_1(1)\beta(1)\ \psi_1(2)\alpha(2) \right)$$

with ψ being the orbital, α and β the spin-up and spin-down electron configurations, and $2^{-0.5}$ the normalization constant. The Hartree-Fock energy (E_{HF}) can be obtained by sandwiching the Hamiltonian operator between this wavefunction on the right and its complex conjugate on the left, dividing the resultant expression by the same quantity sans Hamiltonian operator, and integrating over all spatial and spin coordinates.

$$E_{HF} = \frac{\int \Psi^* \hat{H} \Psi \, d\tau}{\int \Psi^* \Psi \, d\tau}$$

Figure 1.1 – Hartree-Fock energy expression

When E_{HF} is minimized, the atomic or molecular orbitals ψ are given, always described in terms of given initial functions known as a basis set. This method's critical flaw is not describing the details of electron-electron interaction, also known as electron correlation. Each electron is instead treated mathematically as if it were in a mean field of the other electrons rather than feeling the effect of every other individual electron.

A multi-reference wavefunction is constructed using all possible electron configurations a system can adopt and is limited by a selected active space the electrons can populate. The space of orbitals can be divided into three categories based on allowed population. These are doubly occupied orbitals (closed-shell orbitals), active orbitals, and virtual orbitals. Active orbitals are those that may be unoccupied, singly occupied, or doubly occupied, and virtual orbitals are those that are not occupied by electrons. With these categories, it is possible to imagine the need for mathematical formalism that allows description of systems that have chemical character coming not only from one electron configuration, but multiple. The form of the complete active space self-consistent field (CASSCF) wavefunction is a linear combination of individual determinants, each describing a single electron configuration of the system.

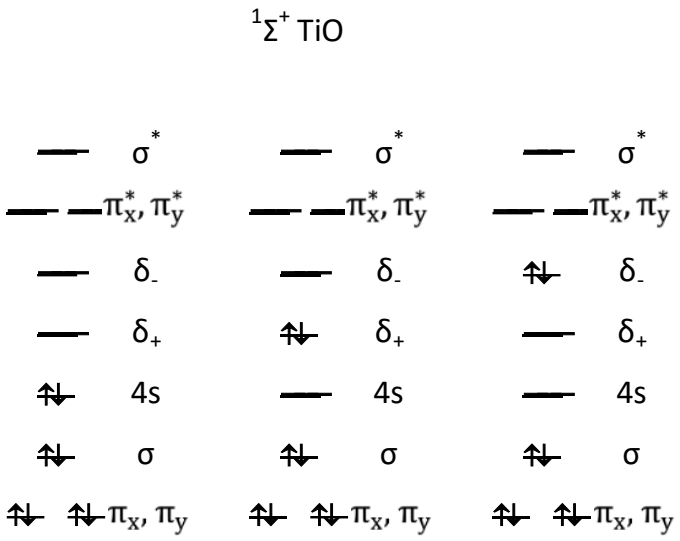

Figure 1.2 – Electron configurations contributing to the $^1\Sigma^+$ state of TiO

The CASSCF energy can be determined in much the same way as E_{HF}, the difference being the structure of the wavefunction. Energy minimization again gives the orbitals, but this time also the coefficients belonging to each determinant within the CASSCF wavefunction. The name of the difference in energy between E_{HF} and E_{CASSCF} is static correlation, and this quantity is important, especially in the case of transition metal systems, which have a large part of their character coming from near-degenerate states. Using the CASSCF formulation of the electronic wavefunction is only the first correction to the HF errors, however, and there are more ways in which to better the approximation of the exact wavefunction.

Multi-reference configuration interaction is the next, more physical, description of the system. The method MRCI (SD) allows single and double replacements of electrons from active orbitals into the virtual orbital space, and minimization of the analogous energy quantity gives the orbitals and coefficients. This is a more physical description of the system, as electrons in nature are free to occupy the virtual orbital space upon the addition of energy into the system.

The Davidson correction to the MRCI energy comes from the issue of the non-size-consistency of the method; that is, the total energy of a system A plus the total energy of a system B is not equal to the total energy of the systems A and B separated by a distance large enough to make interactions of the two systems negligible in effect. The correction attempts to remedy this problem using the correlation energy and the coefficient of the HF wavefunction in the CISD expansion according to the following formula:

$$\Delta E_Q = (1 - a_0^2)(E_{\mathrm{CISD}} - E_{\mathrm{HF}})$$

Figure 1.3 – Davidson correction formula

Discussed previously, the active orbital space is typically constructed with the valence space of the atom or molecule in mind, with adjustment being allowed for computational cost efficiency or chemical reason. This will become a critical discussion in later sections, wherein the active space of the MO_2 system was chosen with a goal in mind, namely that of biasing the system towards showing metal-oxyl character.

Additional post-Hartree-Fock methods

Coupled cluster theory is a theory that remedies some shortcomings of MRCI, namely non-size-extensivity and slow convergence towards the full configuration interaction solution of the Schrödinger solution within a given basis set. This is achieved through an exponential, rather than linear, parameterization of the wavefunction. This parameterization of the wavefunction

ensures additive separability of energies and multiplicative separability of wavefunctions, which in turn yields size-extensivity of the method. Another advantage of the exponential parameterization is that the coupled cluster wavefunction has approximate solutions to all levels of excitation despite truncation of the operator. This feature is what gives CC models faster convergence towards the full CI limit. CCSD(T) is referred to as the proverbial "gold standard," but can only be trusted to live up to its reputation when put to use on single-reference systems. Multireference systems cannot be accurately described by this method. This method also differs from that of previous methods discussed in that it is not variational; the energies given by this method do not give a strict upper bound to the true energy of the system.[1]

CASPT2, or second-order multireference perturbation theory, is an additional theory that was used in this work to benchmark the performance of the MN15 functional. Two variants of this theory were used, the standard multi-state option offered by the MOLPRO15 suite and one with a more contracted configuration space (CASPT2c). This method involves taking a number of CASSCF states and CASPT first-order wavefunctions and adding them together for use as basis functions in an approximate variational calculation. This method is often used where MRCI is not applicable, such as in the case of large molecules up to fifty atoms.[2] CASPT2 is very sensitive to the choice of active space, and the current limit is sixteen active orbitals.

Density functional theory (DFT) is a theory that considers a physical observable, the electron density, in determining the energy and properties of a molecule. The B3LYP and MN15 functionals both belong to the Kohn-Sham family of density functional theory. For this formulation, the exact exchange for a single determinant in the Hartree-Fock energy expression is replaced with the exchange correlation functional. This term can contain not only the exchange energy, but also electron correlation energies (not present in Hartree-Fock theory.

$$E_{HF} = V + \langle hP \rangle + 1/2\langle PJ(P) \rangle - 1/2\langle PK(P) \rangle$$

Figure 1.4 – Form of Hartree-Fock energy expression, where V is the nuclear repulsion energy, P is the density matrix, $\langle hP \rangle$ is the one-electron energy, $1/2\langle PJ(P) \rangle$ is the coulombic repulsion of the electrons, and $-1/2\langle PK(P) \rangle$ is the exchange energy.

$$E_{KS} = V + \langle hP \rangle + 1/2\langle PJ(P) \rangle + E_X[P] + E_C[P]$$

Figure 1.5 – Form of Kohn-Sham energy expression, where $E_X[P]$ is the exchange functional and $E_C[P]$ is the correlation functional.[3]

The functionals used are typically integrals of some function of the electron density and sometimes the density gradient.

The B3LYP functional has the following form:

$$E_{XC}^{B3LYP} = aE_X^{Slater} + (1 - a)E_X^{HF} + b\Delta E_X^{Becke} + cE_C^{LYP} + (1 - c)E_C^{VWN}$$

Figure 1.6 – B3LYP functional[3]

The LYP expression is used for non-local correlation, and the VWN functional III expression is used for local correlation. This functional is very popular, but underestimates

reaction barrier heights. It has been included in the benchmarking study, but due to its reputation, will not be used as the main tool with which reaction energetics are examined.[4]

The MN15 functional, according to Yu et. al, is "a Kohn-Sham global-hybrid exchange-correlation density functional with broad accuracy for multi-reference and single-reference systems and noncovalent interactions," according to their paper.[5] This functional has been tested thoroughly by members of the Miliordos group and others, and has been found to describe the energetics of transition metal systems very accurately. The functional has its roots in the LSDA exchange-correlation energy, but with heavy modification.

Ground and excited states of molecular systems

The lowest-energy arrangement of electrons in optimized orbitals of a molecule is the defining characteristic of the ground state of a molecule. However, these electrons can be excited with added energy to higher-energy electron configurations, and excited states of the system result. Excited states can and do exhibit completely different behavior than that of their ground states, and qualitatively different mechanisms can result from these excited states reacting with the same substrate. Computational methods are a very reliable way to examine the behavior of these excited states and elucidate the reason for different reactivity paths of transition metal catalysts, as prior work of the Miliordos group has shown.[6] Ground and excited states of the transition metal dioxides in this work were examined at the MRCI level of theory to elucidate electronic structure and with DFT to illustrate the energy landscape of C-H bond activation of methane by these dioxides.

Methane, methanol, and transition metal catalysts

One of the Miliordos group's interests is the conversion of methane to methanol.[7,8,9,10] Methane itself is a problematic molecule, threatening future day-to-day life as we experience it today. In the atmosphere, it is a greenhouse gas several times more potent in effect than carbon dioxide. It can, however, be captured and converted to the more economically transportable liquid methanol. Methanol is not only a solution to this carbon capture problem. It is also of interest to anyone in a field that requires raw material or solvent for use in synthetic chemistry. Methanol can be used as a solvent for many industrial reactions, or as a starting material for making a more complex reactant for a synthetic chemist to use. For example, the alternative fuel dimethyl ether and ethylene can both be easily synthesized using methanol as a starting material.

Although there are methods for the conversion of methane to methanol currently in use, these methods are only possible with high temperatures and pressures, and consequently high in cost due to energetic demand. We are interested in showing through quantum mechanical calculations that more energy-efficient methods exist for this conversion, and that they are more economically feasible.

Catalysts that are able to activate the C-H bond of methane are usually non-selective, over-oxidizing the desired product of methanol to carbon dioxide, defeating the purpose of containing this carbon source in liquid form.[11] However, transition metals have low-lying excited states, and their oxides are very versatile when considering C-H bond activation.[12,13] First- and second-row transition metal (TM) oxide catalysts have been recognized as effective and selective converters of methane to methanol (MTM), and theoretical studies of these molecules and their charged species have given insights into their mechanisms.[13,14,15,16] Iron oxide was one of the

first transition metal oxide catalysts to be examined for this purpose due to its abundance and low cost, and the role of NbO and ZrO as a catalyst for MTM conversion was elucidated by other members of the Miliordos group.[9,15,16] Transition metal oxides, their cations, and their anions have been the focus of the group in the recent past.

Rather than continuing exploration of the space of monoxides, this work is the first consideration of the electronic structure of transition metal dioxides and their ability to activate the C-H bond of methane. Understanding the electronic structure of these dioxides offers insight into how the activation of the C-H bond occurs, and this work will pave the path for the further aim of elucidating the complete narrative of the TM dioxides and their role in MTM conversion.

Titanium was chosen as the first metal to be examined due to its relative abundance as well as its low cost when compared to other candidate metals. Vanadium and chromium, titanium's neighbors to the right on the periodic table, have also been examined in order to determine the effect of the metal identity on the electronic structure of the metal dioxide as well as on the ease of C-H bond activation. These systems have been examined with quantum mechanical calculations to show that neutral titanium dioxide, vanadium dioxide, and chromium dioxide are all able to activate the C-H bond of methane, which is the most critical step in the conversion of methane to methanol.

Methane, while important in its own right, offers a computationally friendly case when considering the dioxides' ability to activate C-H bonds in general. Smaller molecular systems are an excellent choice when using more expensive methods such as MRCI, and this is precisely the case with this work. Methane can be used as a case study to which further work can be compared when considering C-H bond activation in systems of a larger size.

Metal-oxo versus metal-oxyl character

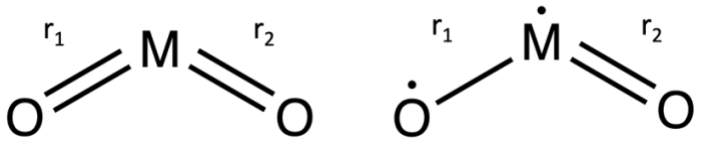

Figure 1.7 – Lewis structures of metal-oxo and metal-oxyl systems

Metal-oxygen bonds can be classified into two different categories based on bond length and electron localization across the bond. Metal-oxo species are made of an oxygen atom and a metal atom connected by a double bond. These have relatively short bond lengths. Metal-oxyl species are made of an oxygen atom and a metal atom as well, but they are connected only with a single bond. This species has one unpaired electron on the oxygen atom and one unpaired electron on the neighboring metal atom, and has a longer bond length than that of an analogous metal-oxo species. We are interested in determining whether or not these dioxides have metal-oxyl character in low-lying states. The metal-oxyl unit allows for much lower energetic barriers for the activation of the C-H bond, which is much more preferable. This presence of this moiety would allow for less energy-intense methods to be used for catalysis.[17,18]

Methods

Reference CASSCF wavefunctions for TiO were defined by distributing the metal $4s^2 3d^2$ and oxygen $2p^4$ electrons to 9 orbitals, which included the 4s of Ti, the five 3d orbitals of Ti, and the three 2p orbitals of O. The remaining lower-energy orbitals (n=1-3 s orbitals of Ti, n=2,3 p orbitals of Ti, n=1,2 s orbitals of O) were enforced to be doubly occupied. These reference wavefunctions were used as an initial guess for all multireference methods (CASPT2, MRCI). Hartree-Fock wavefunctions were used as the initial guess for the CCSD(T) and DFT methods. CASPT2, MRCI, and CCSD(T) methods were also run with a subset (3s orbital of Ti, the 3 3p orbitals of Ti, and the 2s of O) of core orbitals correlated, and this procedure in Chapter 2 is notated as C-method.[19,20,21,23]

Reference CASSCF wavefunctions for the MO_2 systems are analogous to that of TiO with one significant difference. They were defined by again distributing the metal $4s^2 3d^2$ and second oxygen $2p^4$ electrons to 9 orbitals, which included the 4s of Ti, the five 3d orbitals of Ti, and the three 2p orbitals of the second O. The three 2p orbitals of the first O, once active, are now enforced to be doubly occupied. The remaining lower-energy orbitals (n=1-3 s orbitals of Ti, n=2,3 p orbitals of Ti, n=1,2 s orbitals of O) are also enforced to be doubly occupied, just as with the monoxide case.

This has the effect of excluding from the active space the orbital describing one σ bond between the metal and one of the two oxygen atoms, but including the other orbital of the same type. We are interested in the chemistry of one oxygen atom, but not the second, with the one oxygen atom being considered primarily as a ligand and not catalytically active. This biased view of the metal dioxide system allows us to examine the electronic structure of a system with

one oxo ligand and one oxyl ligand. Species with metal-oxyl character have been shown to have more of an ability than metal-oxo units to activate the C-H bond by other members of the Miliordos group.[15,16]

The same basis sets were used for electronic structure determination and for reactivity. The cc-pVTZ basis set was used for Ti, V, Cr, C, N, and H atoms, and the analogous but augmented basis set aug-cc-pVTZ was used for the O and Cl atoms.[23,24] Metal-oxygen and metal-chlorine bonds are polarized toward oxygen and chlorine, and this additional augmentation was necessary to more accurately describe this phenomenon.

The Gaussian16 package was used for all DFT and CCSD(T) calculations, and the MOLPRO15 suite was used for MRCI and CASPT2.[25,26-28]

Chapter 2 : TiO - benchmarking

Background

Titanium monoxide was our first subject of interest in our journey toward understanding transition metal dioxide chemistry. Understanding the behavior of the analogous monoxide system was the key to elucidating the electronic structure of the dioxide system. In addition to this, exploring the electronic structure of the lowest energy states of TiO in detail allowed the opportunity to benchmark the DFT functional MN15 for its performance against methods of known high accuracy.[5] MN15 was previously benchmarked for transition metals by Dr. Khan.[7] He showed MN15 to be capable of accurately describing the energetics of transition metal systems, and that geometric accuracy of solutions given by this functional have little correlation with the energetic accuracy.[7] The portion of work relating to reactivity is concerned primarily with giving accurate energetic data rather than geometric data, so the problem of MN15 giving slightly less accurate geometric results is able to be overlooked. Previous work by Dr. Miliordos showed TiO to have three well-separated low-lying states, being the ground state X $^3\Delta$, first excited state a $^1\Delta$, and second excited state d $^1\Sigma^+$.[6] Three different types of states are represented here, with the ground state being a triplet, the first excited state an open-shell singlet, and the second excited state a closed-shell singlet.

Absolute energies

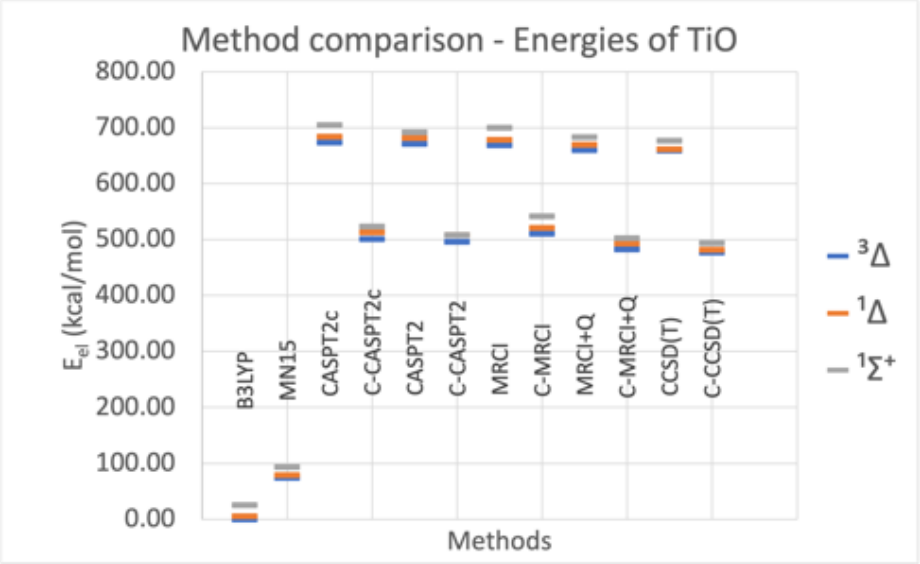

Figure 2.1 – Absolute electronic energies of lowest three states of TiO, shifted so that the B3LYP energy of $^3\Delta$ TiO = 0.

DFT gave qualitatively different absolute energies for the three states of TiO than other methods considered in the benchmarking study. Energies given by DFT are lower than the limit of other methods due to a difference in the way the methods are formulated. DFT solutions approach the minimum of an empirically derived functional as the basis set is extended, whereas the other methods tested approach the minimum of the Hamiltonian. Correlation of the n=3 orbitals of Ti and the 2s orbital of O gives a predictably consistent drop in energy of about 0.27 Hartree. Similar differences between the energy values of states across methods can be observed between these systems, and this is more easily visible when comparing excitation energies.

However, we can see that the energetic separation of states given by MN15 is comparable to that given by C-MRCI+Q and C-CCSD(T).

Bond lengths

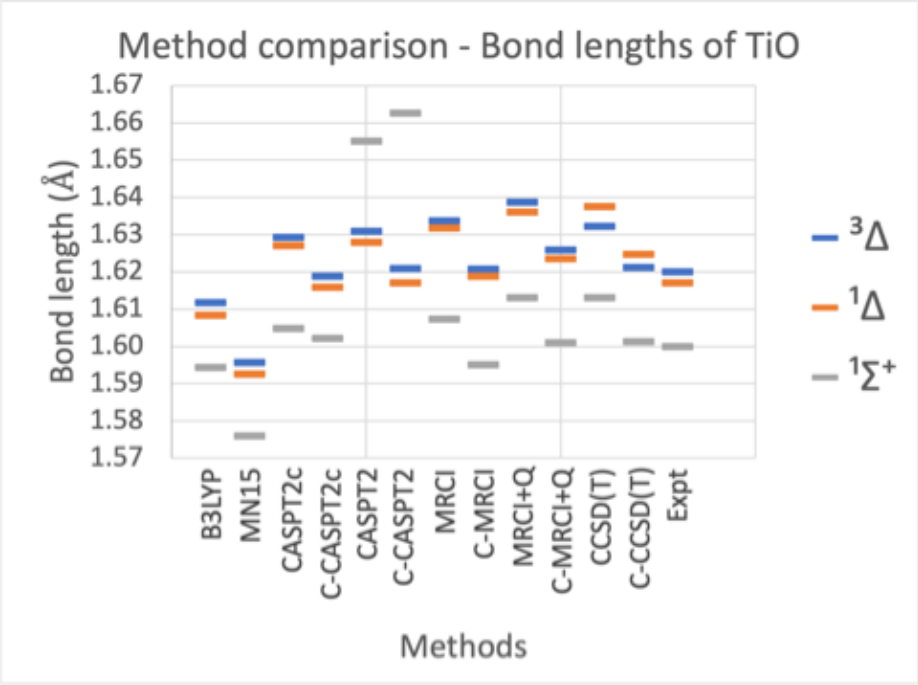

Figure 2.2 – Bond lengths of lowest three states of TiO

Correlation of the same subset of core orbitals consistently correlates with a decrease in the bond length of the system, regardless of multiplicity or spin. The only exception to this trend is that CASPT2 reports an increase of the bond length of the $^1\Sigma^+$ state with correlation of the subset of core orbitals. When considering relative changes in bond length between states rather than absolute bond lengths, there are similarities in the performance of all methods with the exception of CASPT2, which does not describe the system correctly when comparing with the

experimentally observed ordering of states by bond length. DFT characteristically underestimates bond lengths in general, but the values given by B3LYP are very close to that of experiment. Although MN15 performs more poorly than B3LYP in terms of accurate reporting of bond lengths, this has no correlation with the accuracy of energetic data given by MN15, and is not a reason to disregard MN15 as a reliable functional for description of energetics.

Excitation energies

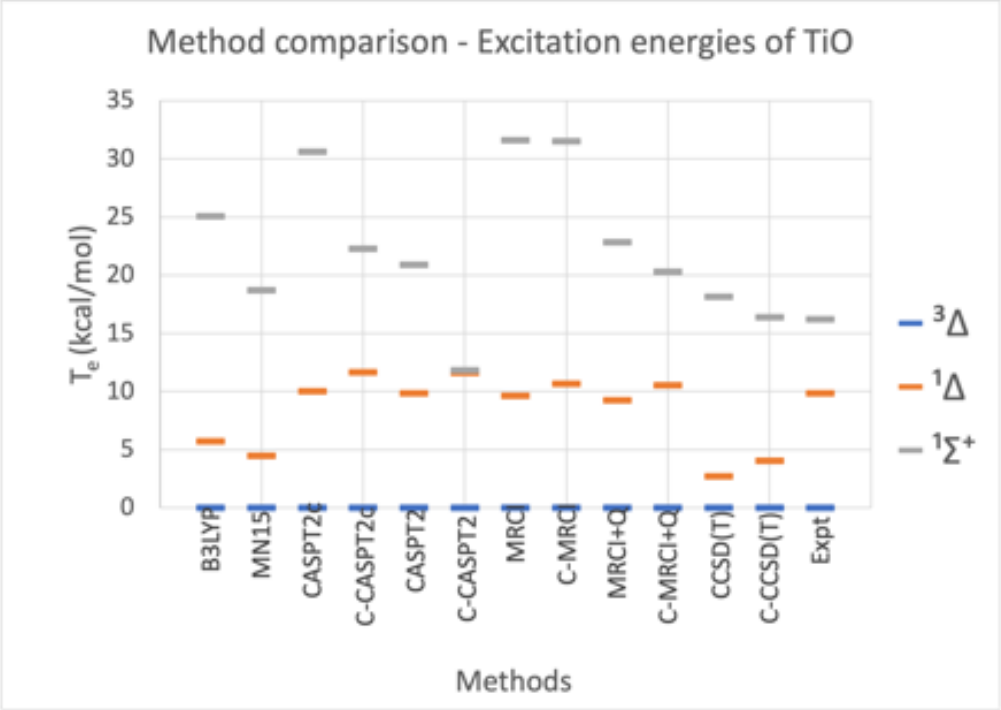

Figure 2.3 – Excitation energies of lowest three states of TiO

Correlation of the same subset of core orbitals raises the reported energy needed to excite TiO to its $^1\Delta$ state, but lowers the energy needed to excite TiO to its $^1\Sigma^+$ state.

We see that when comparing with experimentally derived values for excitation energies: MRCI has good agreement in terms of excitation energy for the $^1\Delta$ state, MN15 and C-CCSD(T) both have good agreement in terms of excitation energy for the $^1\Sigma^+$ state, PT and CI methods are all within 2 kcal/mol of the experimentally derived value for excitation energy for the $^1\Delta$ state, and MRCI grossly overestimates the excitation energy to the $^1\Sigma^+$ state, and only gets marginally better at reproducing experimentally measured values with correlation of the subset of core orbitals and inclusion of the Davidson correction. When comparing computational methods: MN15 has good agreement with C-CCSD(T) when reporting excitation energy for the $^1\Delta$ state, MN15 has good agreement with CCSD(T) when reporting excitation energy for the $^1\Sigma^+$ state, C-CASPT2c performs similarly to MRCI+Q, and CASPT2 performs similarly to C-MRCI+Q for the $^1\Sigma^+$ state. MN15 gives very high level of theory results for excitation energies, matching CCSD(T) in performance for these systems. Single-reference methods like CC are found, however, to be untrustworthy in accurately reporting excitation energies for these systems, which have been shown to have multireference character.

Conclusions

MN15 is not to be trusted with reporting experimentally accurate geometries or precise absolute energies. However, the functional does captures energy differences between states well and matches answers given by trusted methods.

Chapter 3 : Journey to the structure of TiO_2

First examination – scan at linear geometries

Originally, we had imagined the metal dioxide systems to have linear ground states, with additional electrons being distributed to the δ orbitals of the metal. With this naïveté, we constructed scans of the potential energy surfaces of linear TiO_2 in which the bond lengths r_1 and r_2 were varied, with the angle fixed at 180 degrees. At the CASSCF level of theory, no clear geometry corresponding to an energetic minimum was found for the ground or excited states of TiO_2. The resulting surfaces were very flat, and these results can be seen in the following figure. It was clear that exploring variation of the angle was necessary.

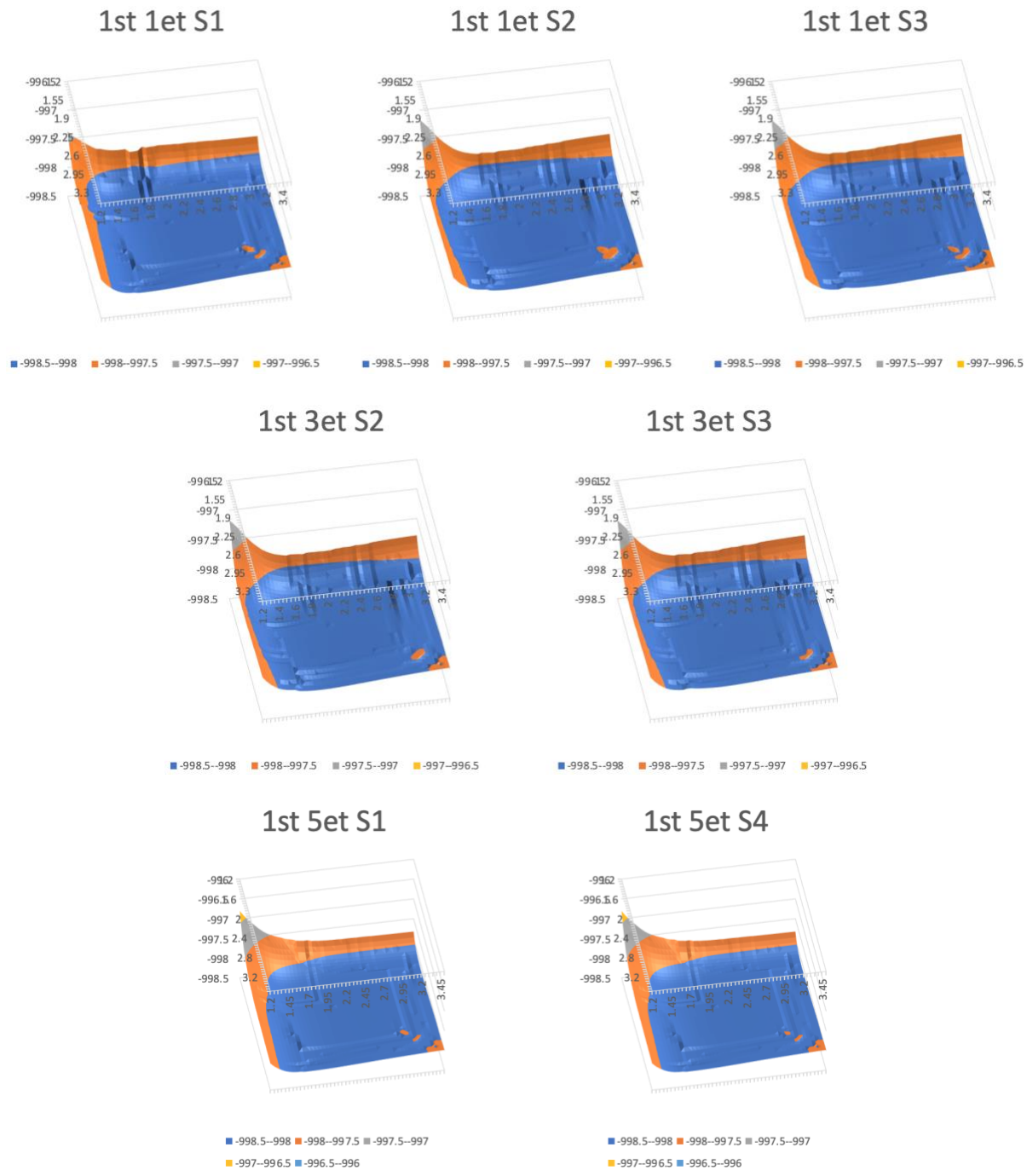

Figure 3.1 – Energies (Hartree) of linear TiO_2 with varied r_1, r_2 (Å)

Second examination –2-D scan with varied bond lengths and angle

The next scan constructed involved varying the angle from 110 to 180 degrees, and the two bond lengths were varied in tandem. Both bond lengths were set to a value of 1.7 Å (intermediate of expected metal-oxo and metal-oxyl bond lengths), and following steps were constructed by adding 0.1 Å to r_1 and subtracting the same value from r_2. These scans were run at the CASSCF and MRCI levels of theory, but results were similarly uninformative with the potential energy surfaces being sloped, but not having a clear minimum. Shorted bond lengths are clearly favored, but no clear preference for an angle was clear for any state considered. A sample of these scans can be viewed in the figure below.

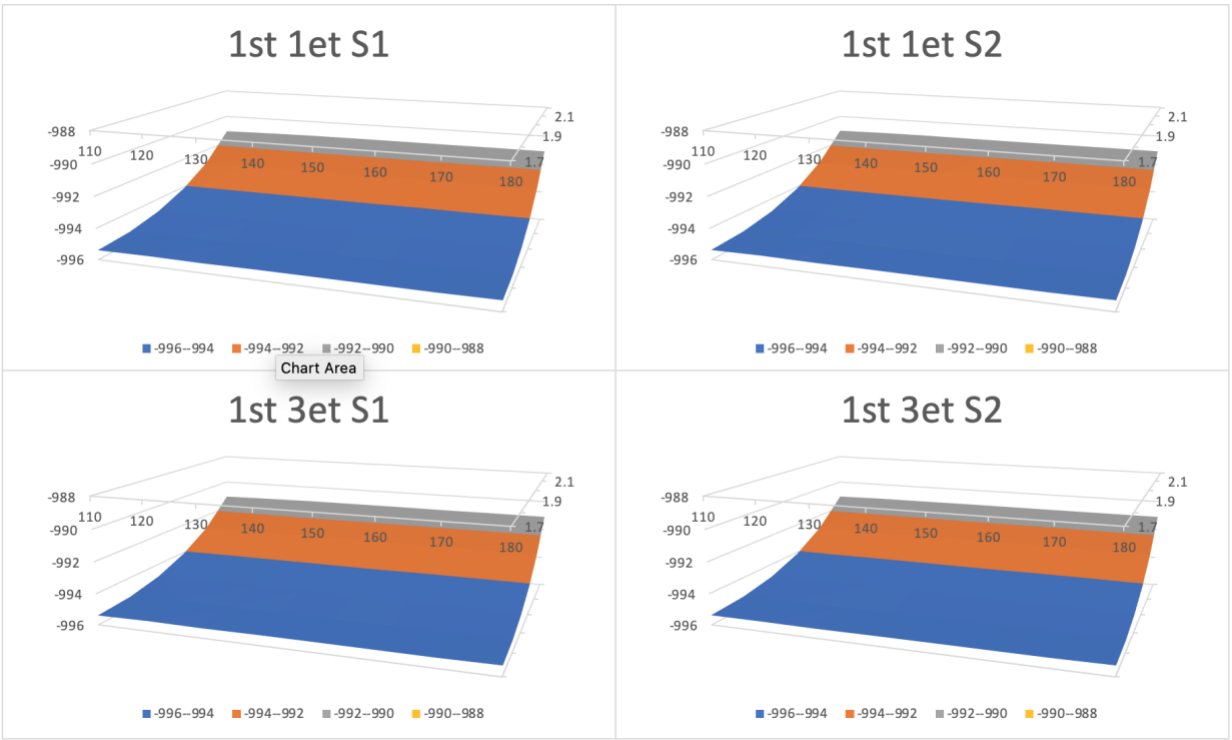

Figure 3.2 - Energies (Hartree) of bent TiO_2 with varied r_1, r_2, φ (Å, deg)

Third examination – DFT results

MN15	1et	3et
r_1 (Å)	1.626	1.600
r_2 (Å)	1.626	1.857
φ (deg)	113.3	111.3
E (Hartree)	-999.86219	-999.78451

Figure 3.3 – Geometric data and energies of lowest-energy singlet and triplet of TiO_2

DFT calculations with the MN15 functional were run with a wide range of initial geometries, and the global minimum for the lowest energy singlet and triplet were found. The reason for the nonlinear geometry was puzzling at first glance, but became more clear when considering the approach of one oxo ligand to the already-formed TiO unit.

Formation of ground state

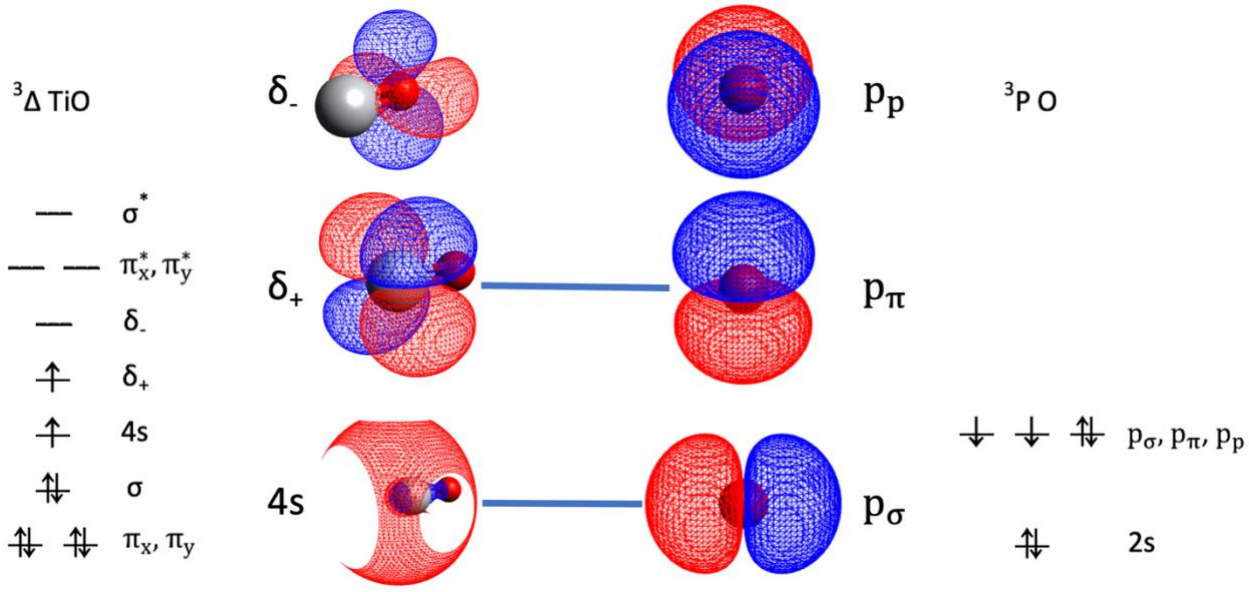

Figure 3.4 – Orbital diagrams and occupations of $^3\Delta$ TiO and ^{3}P O and bonding scheme to form the ground state of TiO_2

Titanium oxide, when in its ground state electron configuration, is a $^3\Delta$, with one electron in an orbital identifiable as the 4s orbital of Ti and another electron in the δ_+ orbital localized on Ti.[6] Oxygen, when in its ground state electron configuration, is a ^{3}P, with two electrons in one 2p orbital and one electron in each of the remaining two 2p orbitals.[29] Here we have denoted the 2p orbitals with labels σ, π, and p (for the orbitals responsible for creating a σ and π bond, and for the perpendicularly-oriented 2p orbital) rather than using the standard x,y,z set. If both unpaired electrons of TiO have α spin and both unpaired electrons of O have β spin, then the ground state of TiO_2 can be formed as follows, but only with an approach at an angle. The p_σ orbital is the 2p orbital of oxygen that will have maximum orbital overlap with the 4s of Ti on approach, forming

a σ bond. The p_π orbital is the 2p orbital of oxygen that will have maximum orbital overlap with the δ_+ orbital of TiO on approach, forming a π bond. The p_p orbital is the 2p orbital of oxygen that will have no significant orbital overlap with the next-highest energy orbital, the δ_-. If this approach were linear, then there would be net zero orbital overlap between the δ_+ and p_π orbitals, creating a less stable product than the product of the angled approach, in which a π bond would also result. An approach at an angle allows this product to form, and this geometry must be kept in order to keep this bonding scheme.

Higher-energy states

When considering stability of excited states of TiO_2, we must consider all possible electron configurations of TiO and O, especially those low in energy. For the TiO unit, we consider that two of titanium's four valence electrons are now in bonding pairs with the first oxygen atom, forming one σ and one π bond. This leaves two unpaired valence electrons free to occupy what orbitals they please. These nonbonding electrons have two available low-energy configurations capable of making bonds with the second oxygen: $4s^1\delta_+^1$ and $4s^1\delta_-^1$. For the approaching O atom, there are three configurations available to it: $2p_\sigma^1 2p_\pi^1 2p_p^2$, $2p_\sigma^1 2p_\pi^2 2p_p^1$, and $2p_\sigma^2 2p_\pi^1 2p_p^1$.

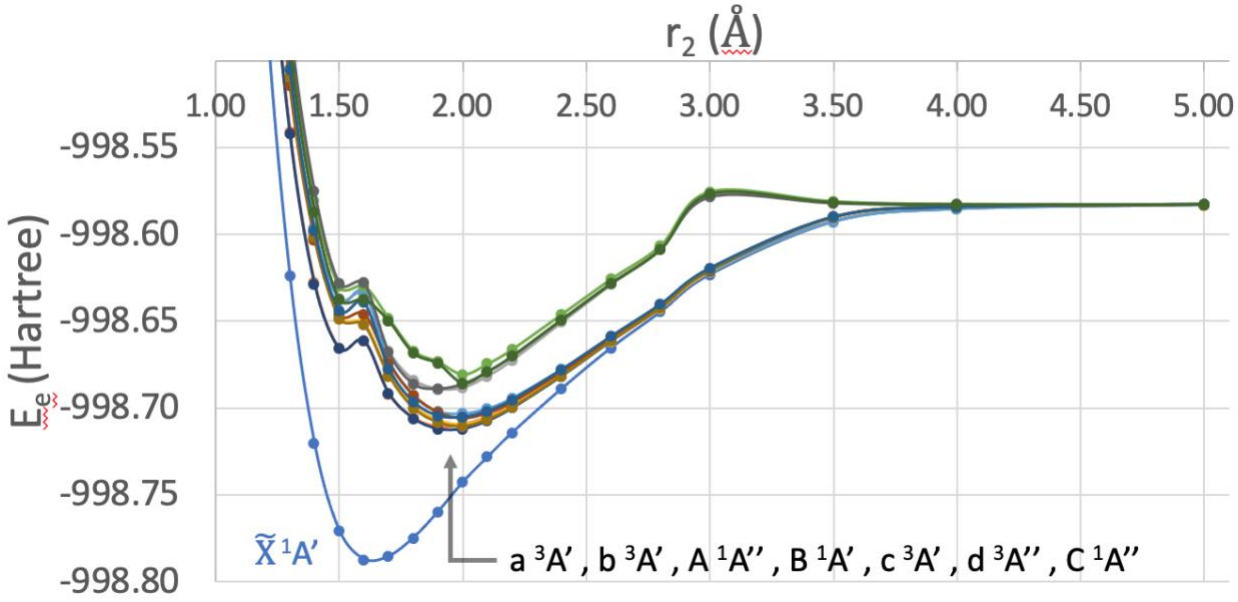

Figure 3.5 – Potential energy curves of lowest twelve states of TiO_2

Potential energy curves were generated at the MRCI level of theory for the approach of the second oxygen to the TiO unit by fixing r_1 to 1.65 Å, φ to 113 degrees, and varying r_2 from 1.1 to 5 Å. One low-lying state followed by a band of seven states was observed, with higher-energy states above the aforementioned band. The ground state of TiO_2 was found to have a shorter r_2 equilibrium bond length compared to the states in the band of seven states above it.

The formation of the ground state singlet has already been discussed, with electron configuration upon approach being Ti:$4s^1\delta_+^1$ O:$2p_\sigma^1 2p_\pi^1 2p_p^2$, with electron spins in bonding orbital pairs $4s2p_\sigma$ and δ_+2p_π being complementary [e.g. $4s(\alpha)2p_\sigma(\beta)$]. The next seven states correspond to varying orbital occupations that only result in a single σ bond being formed between Ti and the approaching O, with no π bond being formed. These states correspond with different occupations of the various p and d orbitals available, with the exception of the $2p_\sigma$ of the approaching O atom being doubly occupied. All of these orbital occupations are listed in the

following table. Four of these states correspond the other δ orbital being filled, but this does not come with an energetic jump due to the near-degeneracy of these δ orbitals. Higher states of TiO_2 correspond to the $2p_\sigma$ orbital of the approaching O being doubly occupied. In this case, a σ bond cannot be formed between the approaching O and the TiO unit, which is energetically unfavorable.

Term Symbol	Orbital occupations		Description
	TiO	O	
^{1,3}A’	$s^1\delta_+^1$	$p_\sigma^1\ p_\pi^1 p_p^2$	1et: GS. σ, π. 3et: only σ.
^{1,3}A’’	$s^1\delta_+^1$	$p_\sigma^1\ p_\pi^2 p_p^1$	Not as bound. Only σ.
^{1,3}A’’	$s^1\delta_-^1$	$p_\sigma^1\ p_\pi^2 p_p^1$	Not as bound, E.S. TiO, only σ.
^{1,3}A’’	$s^1\delta_-^1$	$p_\sigma^1\ p_\pi^1 p_p^2$	Not as bound, E.S. TiO, only σ.
^{1,3}A’	$s^1\delta_+^1$	$p_\sigma^2\ p_\pi^1 p_p^1$	Repulsive
^{1,3}A’	$s^1\delta_-^1$	$p_\sigma^2\ p_\pi^1 p_p^1$	Repulsive

Table 3.1 – Possible orbital occupations of TiO and O, Term symbols and descriptions of resultant systems on approach

Chapter 4 : Electronic structure of TiO_2

Ground state

MRCI	$-E_e$ (Hartree)	r_1	r_2	φ	ω_1	ω_2	ω_3
$\tilde{X}\ ^1A'$	998.80728	1.639	1.660	113.394	320.15	927.95	1059.65

Table 4.1 – Electronic energy (E_h), bond lengths (Å), angle (deg), frequencies (cm^{-1}) of ground state TiO_2

At the MRCI level of theory and with the biased active space, the ground state of TiO_2 was found to be the X $^1A'$ state, having near-equivalent bond lengths. The ground state is non-linear, having an angle of 113°. The bond lengths would be equivalent with an unbiased active space, and this is clear from the results given by MN15. We see that our uncertainty in bond length with this method is then ±0.02 Å. The electrons of TiO_2 preferentially localize on the oxygen atoms in the ground state electron configuration, filling σ and π orbitals polarized toward the oxygen atoms. Both oxygen atoms retain their formal charge of -2, and along with it their oxo character. The ground state of TiO_2 has a doubly occupied σ orbital, π orbital on the plane, and π orbital off the plane. These orbitals can be seen in the following subsection.

Excited states

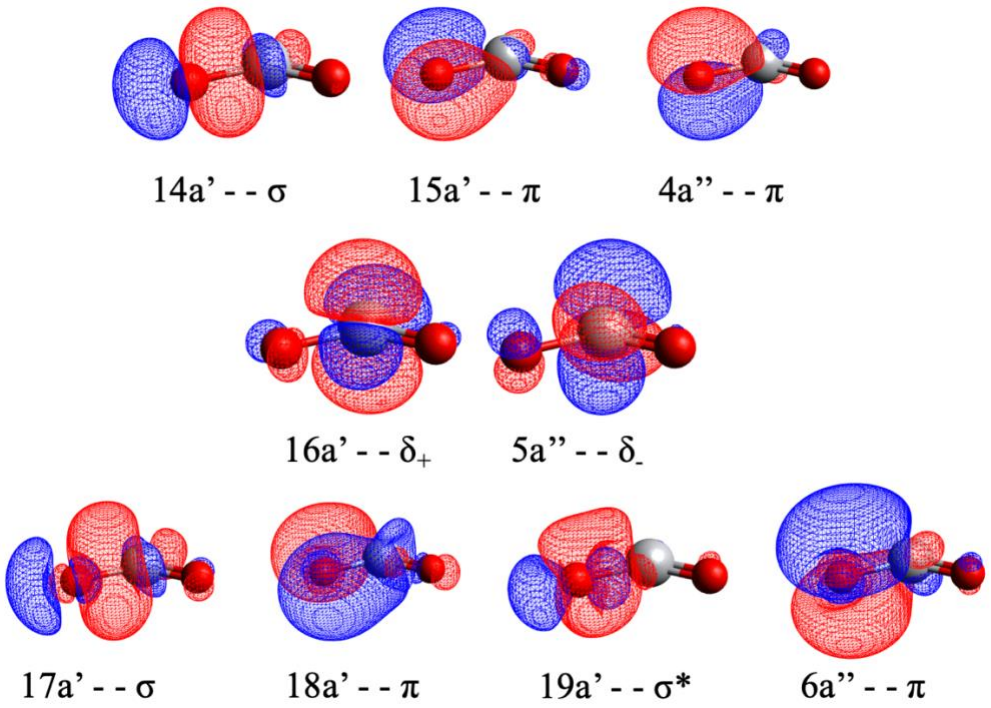

Figure 4.1 – Orbitals of TiO_2

First row: Occupied in ground state, Second row: Occupied in excited states,

Third row: Unoccupied in examined states

State	CI coef.	14a’	15a’	16a’	17a’	18a’	19a’	4a’’	5a’’	6a’’
$\tilde{X}\ ^1A'$	0.95	2	2	0	0	0	0	2	0	0
$a\ ^3A'$	0.98	2	α	α	0	0	0	2	0	0
$b\ ^3A''$	0.98	2	α	0	0	0	0	2	α	0
$A\ ^1A''$	0.70	2	α	0	0	0	0	2	β	0
	-0.70	2	β	0	0	0	0	2	α	0
$B\ ^1A'$	0.59	2	α	β	0	0	0	2	0	0
	-0.59	2	β	α	0	0	0	2	0	0
$c\ ^3A'$	0.97	2	2	0	0	0	0	α	α	0
$d\ ^3A''$	0.98	2	2	α	0	0	0	α	0	0
$C\ ^1A''$	0.69	2	2	β	0	0	0	α	0	0
	-0.69	2	2	α	0	0	0	β	0	0

Table 4.2 – MRCI coefficients and orbital occupations of ground and excited states of TiO_2

Gray coloring: electron removed from orbital, Green text: electron excited to that orbital,

Blue coloring: spin flip with excitation in the orbital

The first seven excited states of TiO_2 involve the removal of electrons from just two π orbitals and the replacement of those electrons into just two δ orbitals. The first excited state involves the removal of an electron from the planar π orbital and its replacement into the δ_+ orbital, with a spin flip that makes this first excited state a triplet. The second excited state involves the removal of an electron from the same orbital and a spin flip as before, but is replaced in the δ_- orbital, again resulting in a triplet. The third excited state is the first state with significant multireference character, and it is an open shell singlet. One of the two primary electron configurations giving rise to this state involves the removal of a β electron from the

same π orbital on the plane into the δ_- orbital, and the other configuration is the spin-reversed case. The fourth excited state is also an open-shell singlet with multireference character. The difference between this state and the previous is the identity of the orbital in which the excited electron is placed; the third excited state involves the placement of the excited electron into the δ_- orbital, and this state instead involves replacement into the δ_+ orbital. The fifth excited state is once again single-reference, and it is a triplet. An electron is removed from the π orbital off the plane and placed into the δ_- orbital, and the spin of the excited electron is flipped from β to α. The sixth excited state, another triplet, involves the removal of an electron from the π orbital off the plane into the δ_+ orbital, with a spin flip from β to α. The seventh and final excited state for which orbital occupations were examined is an open-shell singlet, which again brings with it multireference character. One of the two primary electron configurations giving rise to this state involves the removal of a β electron from the π orbital off the plane and its replacement into the δ_+ orbital, and the other configuration is the spin-reversed case.

In summary, the excited states of TiO_2 are all characterized by the movement of electron density from an oxygen atom to the metal, and all involve the movement of electrons from a π orbital to a δ orbital. Electrons are preferentially excited from the π orbital on the plane before being excited from the π orbital off the plane, which is expected; electrons have much less repulsion when distributed above and below the TiO_2 plane. All singlets (with the exception of the ground state) are open-shell with multireference character, and all triplets found are single-reference and involve a spin flip with respect to the ground state.

Geometries and energies of states

Method	$-E_e$ (Hartree)	r_1	r_2	φ	T_e (kcal/mol)
			$\tilde{X}\ ^1A'$		
MRCI	998.80728	1.639	1.660	113.4	0
MN15	999.86219	1.626	1.626	113.3	0
			$a\ ^3A'$		
MRCI	998.72258	1.627	1.980	135.2	53.15
MN15	999.78451	1.600	1.857	111.3	48.74
			$b\ ^3A''$		
MRCI	998.72114	1.627	1.983	136.2	54.05
			$A\ ^1A''$		
MRCI	998.72096	1.627	1.983	137.3	54.17
			$B\ ^1A'$		
MRCI	998.71464	1.625	1.953	133.3	58.13
			$c\ ^3A'$		
MRCI	998.71528	1.632	2.011	140.6	57.73
			$d\ ^3A''$		
MRCI	998.71481	1.632	2.011	141.9	58.02
			$C\ ^1A''$		
MRCI	998.71357	1.633	2.022	144.6	58.80

Table 4.3 – Geometries and energies of states of TiO_2, with bond lengths in Å, angles in degrees, energy in Hartree, excitation energy (T_e) in kcal/mol

The ground state of TiO_2 has two identical bond lengths according to DFT calculations, and the only reason for MRCI results not mirroring this result is the broken symmetry introduced by the active space. The bond lengths are relatively short compared to that of the remainder of the states' r_2 bond lengths examined at around 1.65 Å. The seven excited states have a greater r_2 than the ground state, increasing by about 0.3 Å. This increase in bond length corresponds with

the bond order decreasing from two to one, indicating the creation of a metal-oxyl moeity. This is consistent with electron density moving away from the oxygen atoms and to the metal. The angle increases with excitation energy to the state.

When comparing the results of MRCI to that of MN15, we see that the methods differ in geometry, but the difference in the reported values for the energy of excitation to the a ^{3}A' state is less than 5 kcal/mol. There are no excited states of TiO_2 that are significantly populated at room temperature.

Chapter 5 : Electronic structure of VO_2

Ground state

MRCI	$-E_e$ (Hartree)	r_1	r_2	φ	ω_1	ω_2	ω_3
$\tilde{X}\ ^2A'$	1093.25887	1.613	1.633	121.589	271.89	961.73	1040.41

Table 5.1 – Electronic energy (E_h), bond lengths (Å), angle (deg), frequencies (cm^{-1}) of ground state VO_2

At the MRCI level of theory and with the biased active space, the ground state of VO_2 was found to be the $X\ ^2A'$ state, and this state has near-equivalent bond lengths. We found that the ground state is again nonlinear with an angle of 121°, slightly greater than that of TiO_2. Again, the bond lengths would be equivalent with an unbiased active space, and this is clear from the results given by MN15. The uncertainty in bond length with this method is again confirmed to be ±0.02 Å.

The electrons of VO_2 preferentially localize on the oxygen atoms in the ground state electron configuration, filling σ and π orbitals polarized toward the oxygen atoms. The additional electron present with the change in metal identity from Ti to V then occupies a δ orbital. Both oxygen atoms retain their formal charge of -2, and along with it their oxo character.
The ground state of VO_2 has a doubly occupied σ orbital, π orbital on the plane, and π orbital off the plane, and one singly occupied δ orbital with most of its density lying exterior to the VO_2 angle.

Excited states

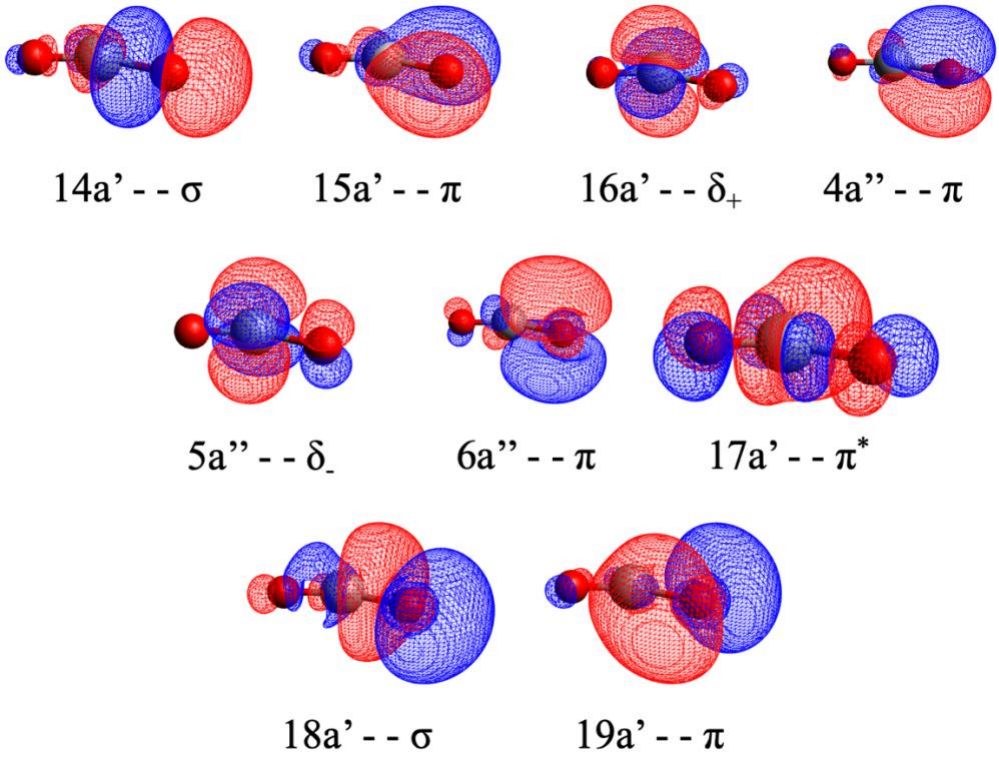

Figure 5.1 – Orbitals of VO_2

First row: Occupied in ground state, Second row: Occupied in excited states,

Third row: Unoccupied in examined states

State	CI coef.	14a’	15a’	16a’	17a’	18a’	19a’	4a’’	5a’’	6a’’
^{2}A'	0.94	2	2	α	0	0	0	2	0	0
A ^{2}A"	0.93	2	2	0	0	0	0	2	α	0
a ^{4}A"	0.98	2	α	α	0	0	0	2	α	0
b ^{4}A'	0.98	2	2	α	0	0	0	α	α	0
B ^{2}A"	0.80	β	2	α	0	0	0	2	α	0
	-0.40	α	2	α	0	0	0	2	β	0
	-0.40	α	2	β	0	0	0	2	α	0
c ^{4}A'	0.82	2	2	α	0	0	0	α	0	α
	0.54	2	2	0	α	0	0	α	α	0

Table 5.2 – MRCI coefficients and orbital occupations of ground and excited states of VO_2

Gray coloring: electron removed from orbital, Green text: electron excited to that orbital,

Blue coloring: spin flip with excitation in the orbital

The first excited state of VO_2, another doublet, involves the removal of an electron from the δ_+ orbital occupied in the ground state to the δ_- orbital. This excitation requires very little energy (7 kcal/mol) compared to the excitation energy required by the remainder of the excited states, which require more than 45 kcal/mol as reported by MRCI. The second excited state is the first quartet, and involves the removal of an electron from the π orbital on the plane and replacement into the δ_- orbital. This is the first instance of movement of electron density both away from an oxygen atom and towards the metal center. The third excited state is another quartet, distinguished from the first triplet by the identity of the orbital from which the electron is removed – the π orbital off the plane. The fourth excited state, the B ^{2}A’’ state, is the first of significant multireference character. The primary electron configuration of this state involves the

removal of an α electron from the σ orbital and replacement into the δ_- orbital. The minor contributions to this state come from the remaining possible cases of spin assignment to the σ orbital and the two δ orbitals. The fifth excited state is the first multireference quartet, with most of its character coming from excitation of an electron from the π orbital off the plane to a higher-energy π orbital off the plane, accompanied by a spin flip. A less significant contribution to this state comes from the simultaneous removal of electrons from the δ_+ orbital and the π orbital off the plane and replacement into the π^* orbital and the δ_- orbital, both of which are localized on the metal, with one spin flip.

In terms of orbitals, the VO_2 system differs from TiO_2 in that it has a qualitatively new π^* orbital populated in one of its excited states. In addition to this, we see the removal of electrons from the σ orbital, which was not seen in the TiO_2 system.

Geometries and energies of states

Method	$-E_e$ (Hartree)	r_1	r_2	φ	T_e (kcal/mol)
			$\tilde{X}\ ^2A'$		
MRCI	1093.25887	1.613	1.633	121.6	0
MN15	1094.39821	1.596	1.596	117.2	0
			$A\ ^2A''$		
MRCI	1093.24818	1.603	1.626	124.1	6.71
			$a\ ^4A''$		
MRCI	1093.18624	1.580	1.947	148.3	45.58
MN15	1094.34682	1.582	1.895	146.4	32.24
			$b\ ^4A'$		
MRCI	1093.18411	1.588	1.978	179.9	46.91
			$B\ ^2A''$		
MRCI	1093.17724	1.582	1.867	180.0	51.22
			$c\ ^4A'$		
MRCI	1093.13233	1.638	2.013	179.9	79.40

Table 5.3 – Geometries and energies of states of VO_2, with bond lengths in Å, angles in degrees, energy in Hartree, excitation energy (T_e) in kcal/mol

The ground state of VO_2, similar to the ground state of TiO_2, also has two identical bond lengths when DFT calculations were run, and the disparity in bond lengths reported by MRCI is once again an artifact of the active space. However, the first excited state of VO_2 has metal-oxo character for both of its bonds as a result of the degree of freedom introduced by the additional electron, now able to populate either the δ_+ or δ_- orbital without a significant rise in energy. When comparing the two lowest states of VO_2 to the remaining states examined, r_2 increases from around 1.62 Å to around 1.95 Å, indicating the appearance of metal-oxyl character with the higher-energy states. The angle also increases with excitation energy, similar to the trend seen

for TiO_2, but with the appearance of linear geometries at high energy states. When comparing the results of MRCI to that of MN15, we see that MN15 has the predicted underestimation of bond lengths. MN15 also reports the excitation energy from the X ^{2}A' state to the a ^{4}A'' state to be 13 kcal/mol less than that reported by MRCI, more than twice the disparity reported for the TiO_2 system.

The electronic structure of the ground and excited states of VO_2 is much more complex than that of TiO_2. VO_2 has more orbitals from which and to which electrons are excited, and there are no analogous doublets and quartets within the examined range of states, unlike TiO_2. The creation of metal-oxyl character is also not limited to electron density moving from π orbitals to δ orbitals, as shown with the states B ^{2}A'' and c ^{4}A'. The first excited state is also a state of doubly metal-oxo character, which differs from the first excited state of the TiO_2 system. Electrons are not preferentially excited from the π orbital on the plane of the metal, instead having a wide range of orbitals from which electrons are removed to populate excited states.

Chapter 6 : Electronic structure of CrO_2

Ground state

MRCI	$-E_e$ (Hartree)	r_1	r_2	φ	ω_1	ω_2	ω_3
$\tilde{X}\ ^3A''$	1193.66064	1.599	1.612	136.647	235.14	959.12	1048.60

Table 6.1 – Electronic energy (E_h), bond lengths (Å), angle (deg), frequencies (cm^{-1}) of ground state CrO_2

At the MRCI level of theory and with the biased active space, the ground state of CrO_2 was found to be the $X\ ^3A''$ state, having near-equivalent bond lengths. Again, the ground state is non-linear with an angle of 136°, the greatest of the three angles found for the ground states of the metals examined. Once again, the bond lengths would be equivalent with an unbiased active space, supported by the MN15 results, and the uncertainty in bond length is not expanded from the established ±0.02 Å.

Just as with the other two metals, the electrons of CrO_2 preferentially localize on the oxygen atoms in the ground state electron configuration, filling σ and π orbitals polarized toward the oxygen atoms before evenly occupying the available δ orbitals. Both oxygen atoms retain their formal charge of -2, and along with it their oxo character, like Ti and V. The ground state of CrO_2 has a doubly occupied σ orbital, π orbital on the plane, and π orbital off the plane and has a singly occupied δ_+ and δ_- orbital, both of which have electrons of α spin. The density of the δ orbitals, for the most part, lies exterior to the CrO_2 angle, just as seen for the VO_2 system.

Excited states

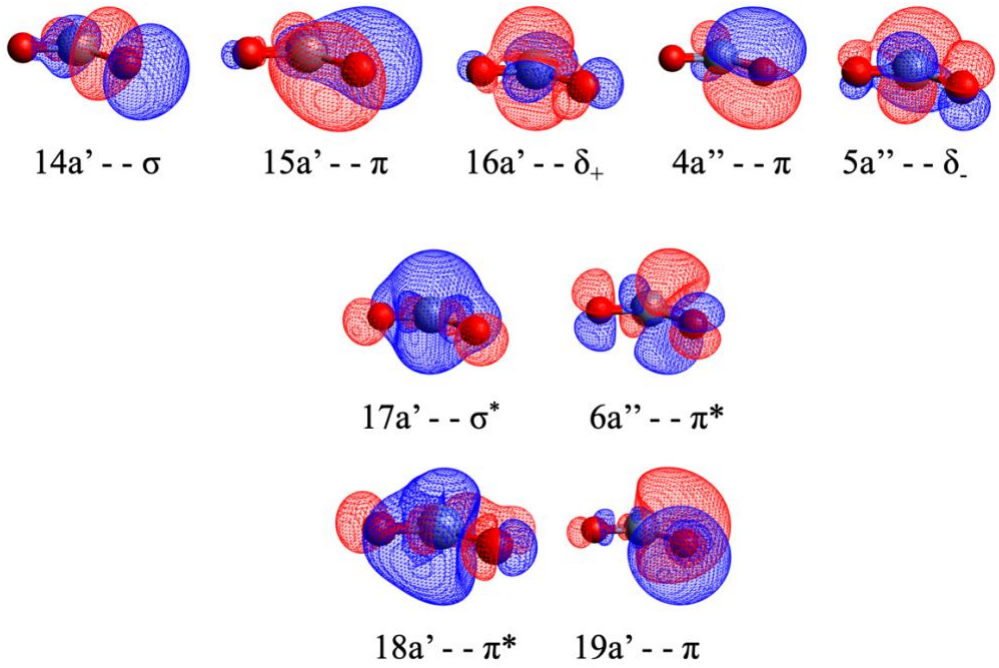

Figure 6.1 – Orbitals of CrO_2

First row: Occupied in ground state, Second row: Occupied in excited states,

Third row: Unoccupied in examined states

State	CI coef.	14a’	15a’	16a’	17a’	18a’	19a’	4a’’	5a’’	6a’’
^{3}A"	0.93	2	2	α	0	0	0	2	α	0
a ^{1}A'	0.92	2	2	2	0	0	0	2	0	0
b ^{1}A"	0.67	2	2	α	0	0	0	2	β	0
	-0.67	2	2	β	0	0	0	2	α	0
A ^{3}A"	0.72	2	2	0	α	0	0	2	α	0
B ^{3}A'	0.69	2	2	0	0	0	0	2	α	α
	-0.42	2	0	2	0	0	0	2	α	α
c ^{5}A"	0.99	2	2	α	0	0	0	α	α	α
d ^{5}A'	0.99	2	α	α	0	0	0	2	α	α

Table 6.2 – MRCI coefficients and orbital occupations of ground and excited states of CrO_2

Gray coloring: electron removed from orbital, Green text: electron excited to that orbital,

Blue coloring: spin flip with excitation in the orbital

The first excited state of CrO_2 is a closed-shell singlet in which the α electron occupying the δ_- orbital is removed and replaced into the δ_+ orbital with a spin flip. The second excited state is the first state in the range of excited states explored that has multireference character. The b ^{1}A" state is an open-shell singlet, the sister singlet of the ground state triplet, and has equal contribution to its electronic state from a spin flip in either the δ_+ or δ_- orbitals. The third excited state is the first excited state triplet, and involves the removal of an electron from the δ_+ orbital and replacement into the σ^* orbital localized on the metal. This orbital is qualitatively different from orbitals seen for TiO_2 and VO_2. The fourth excited state is the second excited state with multireference character, but has unequal contribution from its major electron configurations.

The electron configuration making up the plurality of the state comes from the removal of an electron from the δ_+ orbital and its replacement into the π^* orbital, which is a qualitatively new orbital as well. The lesser, but still significant, contribution to the state comes from the electron configuration in which both electrons are removed from the π orbital on the plane. The beta electron is then replaced into the δ_+ orbital and the α electron is replaced into the π^* orbital. Only the minor contribution involves the movement of electron density away from the oxygen atom and toward the metal center, giving this state minor metal-oxyl character. The fifth excited state is the first quintet, in which an electron is removed from the π orbital off the plane and replaced in its corresponding π^* orbital with a spin flip. This excitation results in movement of electron density from the oxygen atom to a more even distribution across the system, with most of the density on the metal. The sixth excited state is the second quintet, and differs from the first quintet in the identity of the orbital from which the electron is removed. For this state, that orbital is the π orbital on the plane rather than its orthogonal counterpart.

The CrO_2 system is similar to the TiO_2 system in that electrons are not removed from the σ orbital like they are in the VO_2 system for its first six excited states. There is the appearance of the σ^* orbital which distinguishes this system from the prior metals, however.

Geometries and energies of states

Method	$-E_e$ (Hartree)	r_1	r_2	φ	T_e (kcal/mol)
			$\tilde{X}$ ^{3}A"		
MRCI	1193.66064	1.599	1.612	136.6	0
MN15	1194.89910	1.586	1.586	135.3	0
			a ^{1}A'		
MRCI	1193.62674	1.576	1.606	133.0	21.27
			b ^{1}A"		
MRCI	1193.62253	1.587	1.601	132.5	23.91
MN15	1194.86211	1.573	1.573	124.5	23.21
			A ^{3}A"		
MRCI	1193.61417	1.572	1.610	123.7	29.16
			B ^{3}A'		
MRCI	1193.58994	1.643	1.787	126.9	44.36
			c ^{5}A"		
MRCI	1193.57153	1.588	1.927	142.0	55.92
MN15	1194.83734	1.565	1.824	140.5	38.75
			d ^{5}A'		
MRCI	1193.56471	1.584	1.908	135.2	60.20

Table 6.3 – Geometries and energies of states of CrO_2, with bond lengths in Å, angles in degrees, energy in Hartree, excitation energy (T_e) in kcal/mol

All states of CrO_2 up to the first quintet have metal-oxo character in both of their bonds with the exception of the B ^{3}A' state, which has some metal-oxo character coming from its minor CI contribution, but not enough to consider the molecule to have a metal-oxyl unit. The inequality in the bond lengths of the states below the B ^{3}A' state are not a result of oxo character, but of the biased active space, as seen in the other systems. Again, we see underestimation of bond lengths by MN15, but matching excitation energies for the b ^{1}A'' state. DFT and MRCI

disagree by 17 kcal/mol for the excitation energy to the c ^{5}A'' state, which is the largest difference in reported energies seen between the two methods across all systems. There is no correlation between the angle and the excitation energy to the state, which is a new feature not seen with the TiO_2 and VO_2 systems.

The electronic structure of CrO_2 differs from that of prior metals in that when energy is added to the system, electrons are preferentially excited from the δ orbitals rather than the π or σ orbitals, which was seen in Ti and V, respectively. The reappearance of sister states occurs, however, with the a ^{1}A' and b ^{1}A'' states. The creation of metal-oxyl character comes from the removal of electrons from π orbitals and replacement into π* orbitals, which differs from the mechanism of generation of metal-oxyl character for TiO_2 and VO_2.

Conclusions – MO_2 electronic structure

In terms of metal identity, moving from Ti to V to Cr increases the electron count, and each addition electron populates the available delta orbitals evenly. Titanium dioxide has no excited states with low energy separation from that of the ground state, since the only electron removal observed is that from a π orbital polarized towards oxygen, and not a delta orbital. Vanadium dioxide does have one excited state with low-energy separation from the ground state at 6.7 kcal/mol, and this is now possible due to the identity of the orbital from which and to which the first excitation is performed, the δ orbitals of vanadium dioxide. Chromium dioxide has quite a few lower-energy excited states with excitation energies ranging from 21.3 to 44.4 kcal/mol, but no excited states with a separation from the ground state similar to that of the first excited state of vanadium dioxide, all of which lack metal-oxyl character. The appearance of

metal-oxyl character in all three dioxide systems coincides with values for excitation energy to the state at or above 44 kcal/mol, and all states with lower excitation energies exhibit primarily metal-oxo character.

Chapter 7 : Ligand effects

Introduction

The addition of strong-field ligands such as NH_3 has been shown to stabilize high oxidation states of transition metals, which is directly correlated with low oxidation states of their ligands.[9] In contrast, weak field ligands such as Cl have been shown to stabilize low oxidation states of transition metals, which in turn stabilizes metal-oxyl species.[16] Previous work by members of the Miliordos group has shown the ability of ammonia and chlorine ligands to stabilize metal-oxo and metal-oxyl units, respectively, for transition metal monoxides.[16] We seek to discover whether this trend holds for transition metal dioxide systems. First, minima were found for the three dioxide systems in complex with each ligand separately. The ligand-metal distance was then systematically extended and fixed, and all other bond lengths and angles were free to change during the course of the geometry optimization. The r_1, r_2, and energy values were measured for each system from their respective equilibrium ligand-metal distances to a ligand-metal distance of 3.25 Å away from their equilibrium distance, with 17 intermediate points. The ammonia-ligated systems will be discussed first in order of increasing atomic number, and then the same will be done for the chlorine-ligated systems.

Ammonia

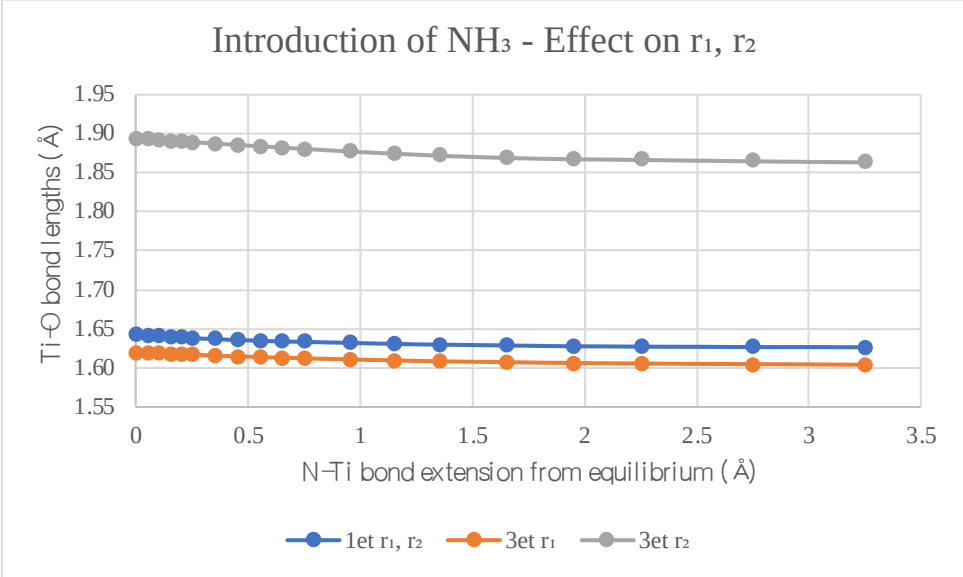

Figure 7.1 – Bond lengths, energies of H_3N-TiO_2 with varying H_3N-Ti distance

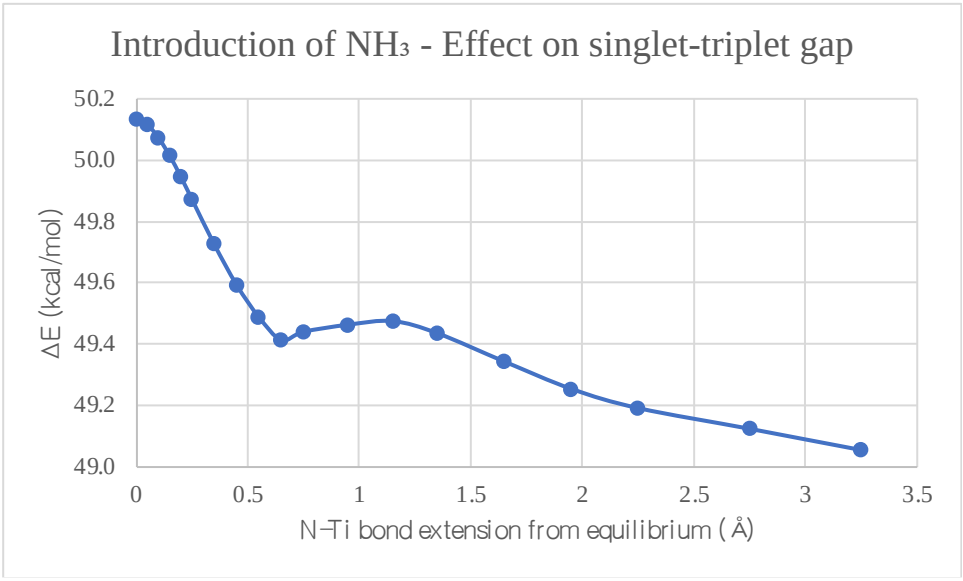

Figure 7.2 – Singlet-triplet gap of H_3N-TiO_2 with varying H_3N-Ti distance

There was a slight increase in both r_1 and r_2 upon ligation with NH_3 when examining both the singlet and triplet systems of TiO_2. The bond lengths of the singlet system extend by 0.016 Å, and the Ti-O bonds of the triplet system extend asymmetrically, with the metal-oxo bond increasing by 0.016 Å and that of the metal-oxyl by 0.029 Å. The singlet-triplet gap of the system increases with decreasing metal-ligand distance until equilibrium, but only by 1.08 kcal/mol.

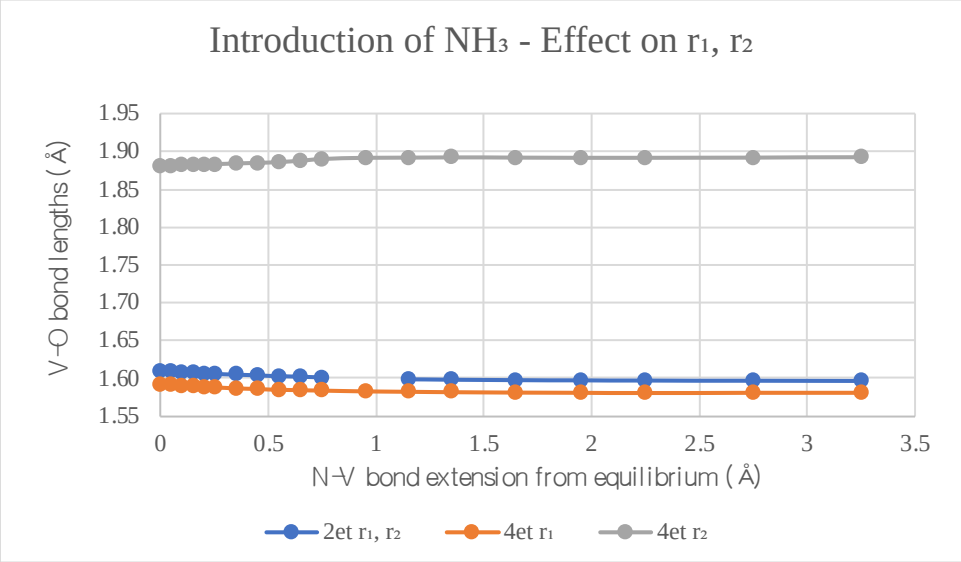

Figure 7.3 – Bond lengths, energies of H_3N-VO_2 with varying H_3N-V distance

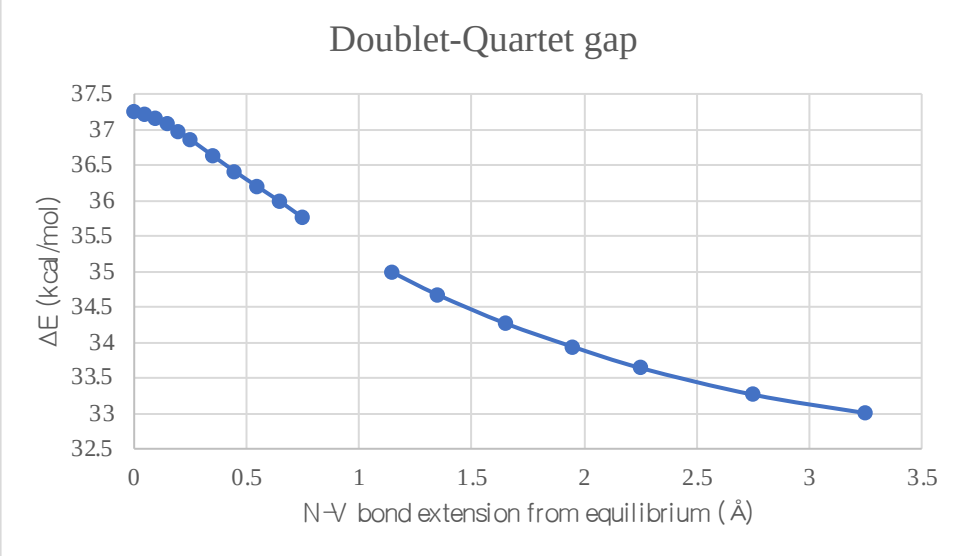

Figure 7.4 – Doublet-quartet gap of H_3N-VO_2 with varying H_3N-V distance

The lowest-energy doublet and quartet states of VO_2 exhibit different behavior upon introduction of NH_3. Both bonds of the doublet system extend by 0.013 Å with ligation of NH_3, which is comparable to the value seen in the low-multiplicity TiO_2 system. The bonds of the quartet system, however, exhibit different behavior, with the metal-oxo bond extending by 0.011 Å and the metal-oxyl bond contracting by 0.011 Å. The doublet-quartet gap of the system increases with decreasing metal-ligand distance until equilibrium, but only by 4.24 kcal/mol.

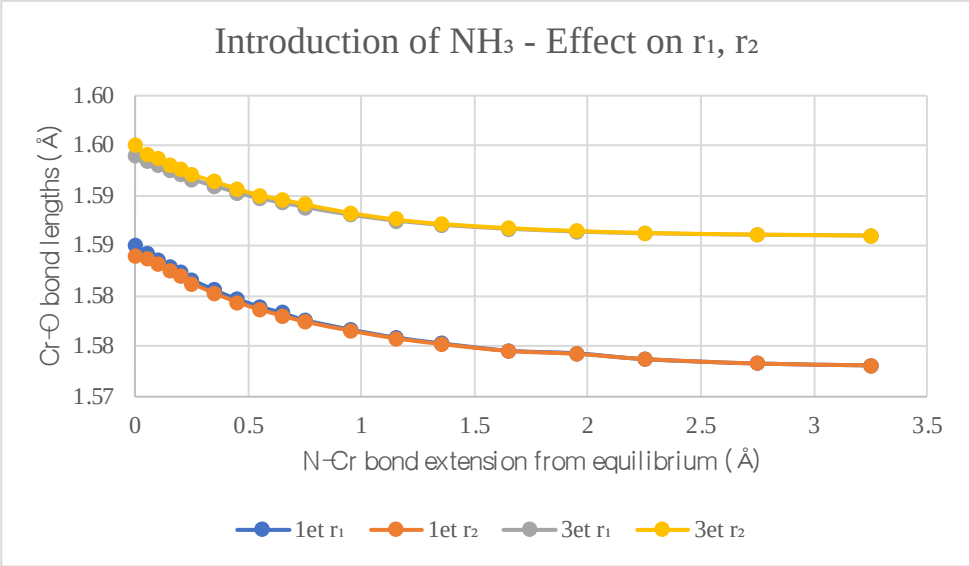

Figure 7.5 - Bond lengths, energies of H_3N-CrO_2 with varying H_3N-Cr distance

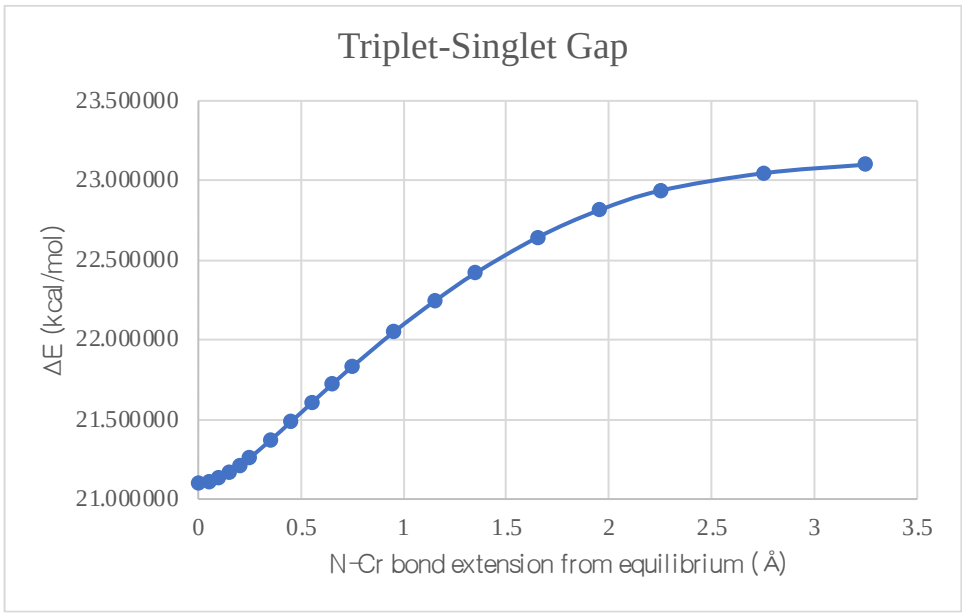

Figure 7.6 - Triplet-singlet gap of H_3N-CrO_2 with varying H_3N-Cr distance

The lowest-energy triplet and singlet states of CrO_2 exhibit similar behavior upon introduction of the NH_3 ligand. The bonds of the singlet both extend, but one by 0.012 Å and the other by 0.011 Å. The bonds of the triplet also both extend, but one by 0.008 Å and the other by 0.009 Å. Although exceedingly small, this also happens to be the first case of unequal bond lengths reported at equilibrium, with both the singlet and triplet systems having a difference of 0.001 Å between the two bonds when NH_3 is at its equilibrium distance. The triplet-singlet gap of the system decreases with decreasing metal-ligand distance until equilibrium, and retains the small energy change across the range of dissociation that was observed in the previous metal dioxide systems with a value of 2.00 kcal/mol.

The expectation was for the introduction of an ammonia ligand to shorten any bonds of metal-oxyl character, but this was not observed. Instead, the bonds were all extended by less than 0.03 Å with the exception of the metal-oxyl bond of VO_2, which contracted with the introduction of the ligand. Clearly, there is no significant perturbation in bond length, which suggests that the introduction of this ligand to the metal dioxide systems would not have a drastic effect on stabilizing mechanisms of C-H bond activation that rely on the presence of metal-oxo character.

Chlorine

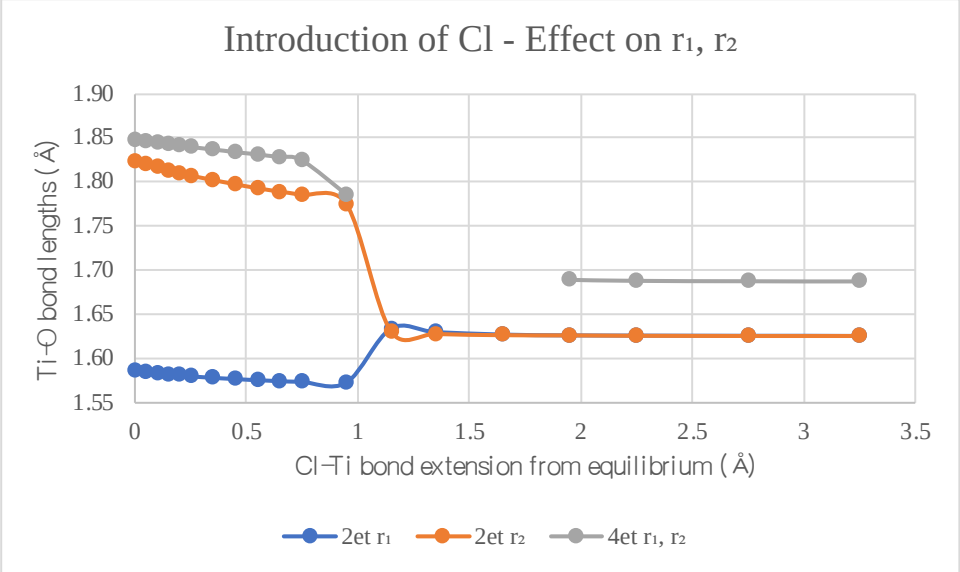

Figure 7.7 - Bond lengths, energies of Cl-TiO_2 with varying Cl-Ti distance

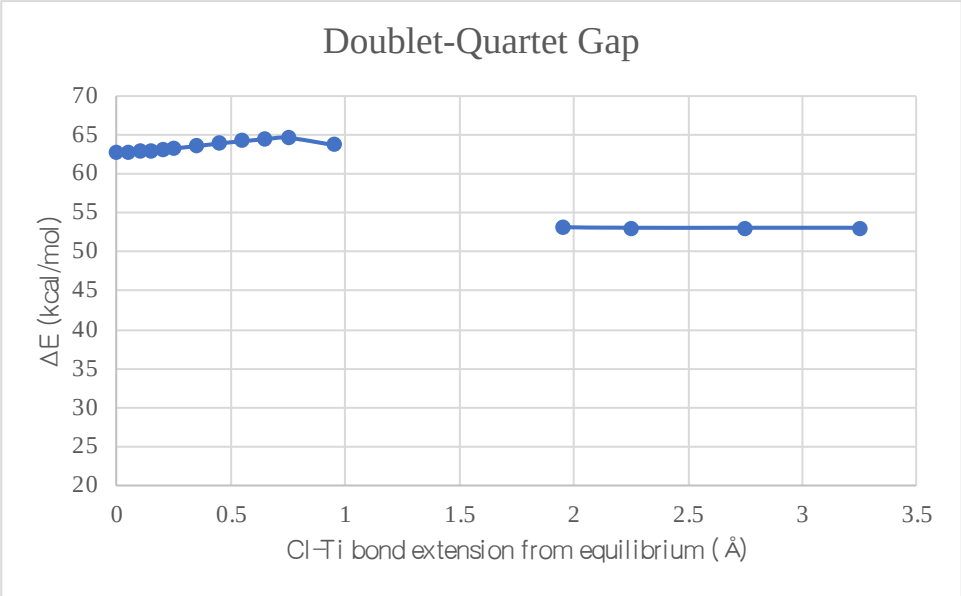

Figure 7.8 – Doublet-quartet gap of Cl-TiO_2 with varying Cl-Ti distance

Upon introduction of Cl to the singlet TiO_2 system, one bond extends to 1.824 Å and the other contracts to 1.587 Å, with both bond lengths beginning with a value of 1.626 Å. The quartet system exhibits different behavior with the dissociation of Cl. The bonds remain equivalent when the Cl ligand is bound at a value of 1.848 Å and decrease in length while remaining equal to a value of 1.688 Å when the Cl ligand is no longer bound. The doublet-quartet gap of the system does not have a consistent trend, first increasing with perturbation from the equilibrium geometry from 62.8 kcal/mol to 64.5 kcal/mol and then dropping to around 53 kcal/mol for the dissociated Cl system. Over the Cl-Ti extension range, the doublet-quartet gap ranges less than 12 kcal/mol. One thing to note is that in the lower-multiplicity system, although the change in bond lengths occurs sharply, the potential energy curve is smooth.

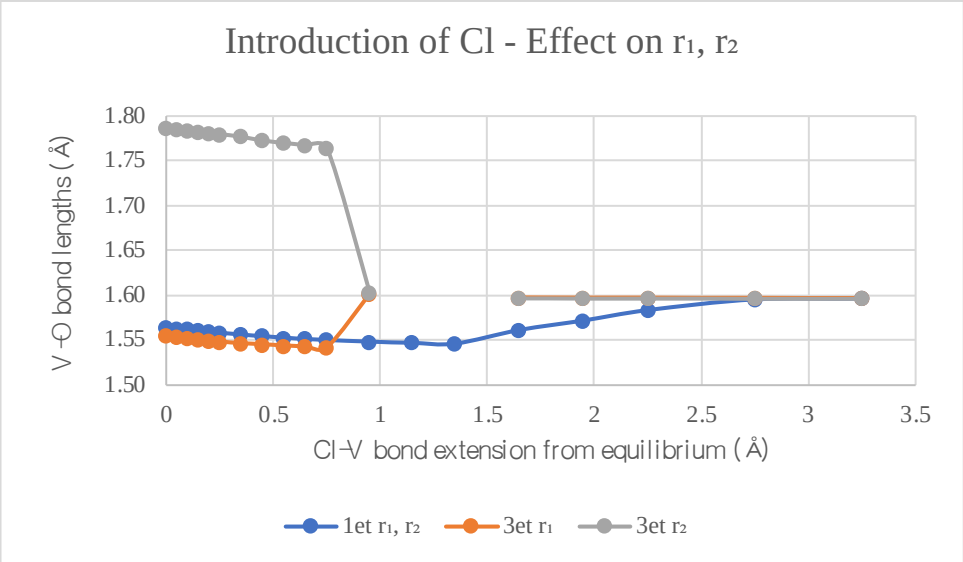

Figure 7.9 - Bond lengths, energies of Cl-VO_2 with varying Cl-V distance

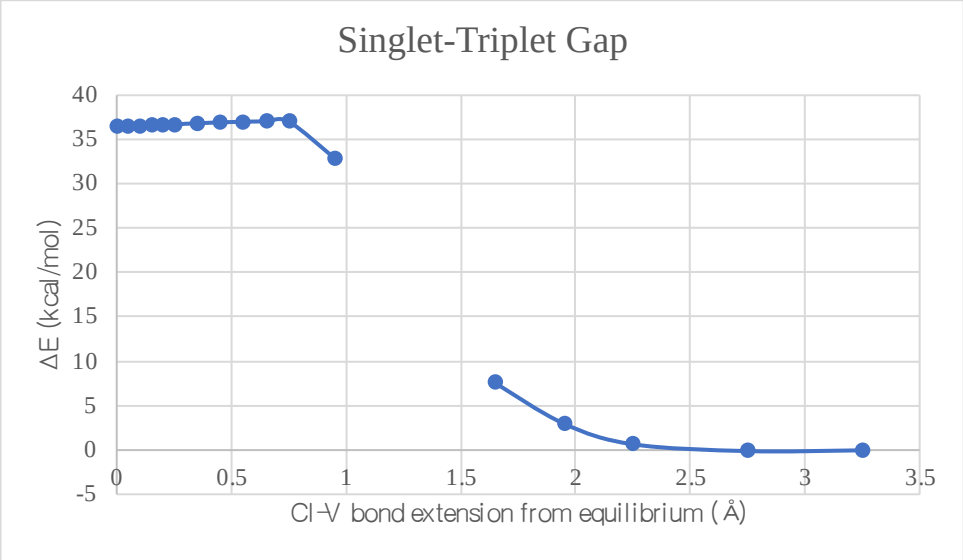

Figure 7.10 - Singlet-triplet gap of Cl-VO_2 with varying Cl-V distance

As the V-Cl distance decreases in the singlet Cl-VO_2 system, the two bonds remain equal. They start at a value of 1.597 Å when the ligand is far from the metal center, then contract to 1.546 Å before extending again to 1.565 Å. The quartet system exhibits different behavior with the dissociation of Cl. Upon introduction of Cl to the quartet VO_2 system, one bond extends to 1.787 Å and the other contracts to 1.555 Å, with both bond lengths beginning with a value of 1.596 Å at large Cl-V distance. The singlet-triplet gap of the system has a value of 36.5 kcal/mol at equilibrium. This value increases slightly to 37.1 kcal/mol with the increase of the Cl-V distance before falling off sharply to zero at a 2.25 Å extension of the equilibrium bond length. Over the Cl-V extension range, the singlet-triplet gap ranges about 37 kcal/mol.

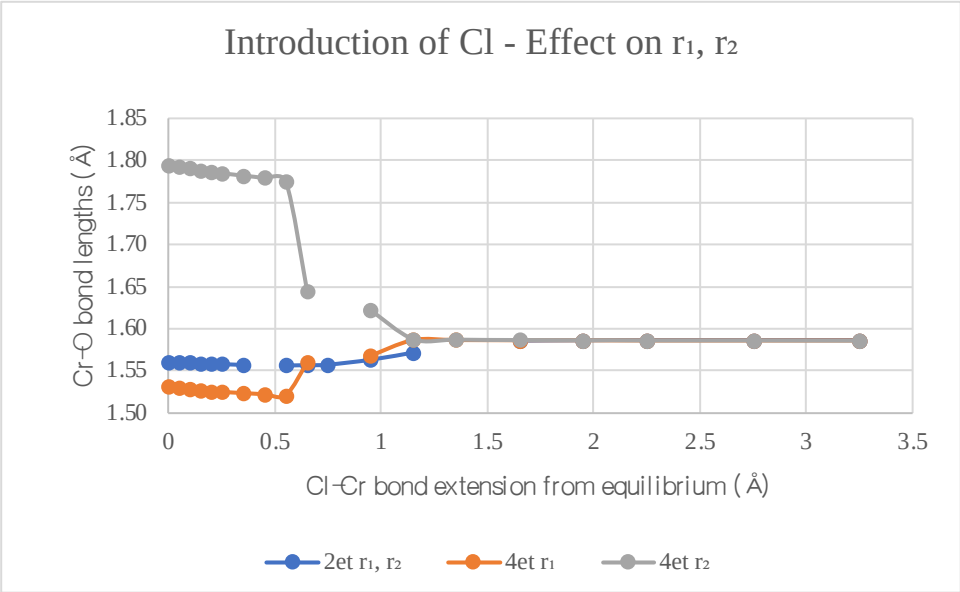

Figure 7.11 - Bond lengths, energies of Cl-CrO_2 with varying Cl-Cr distance

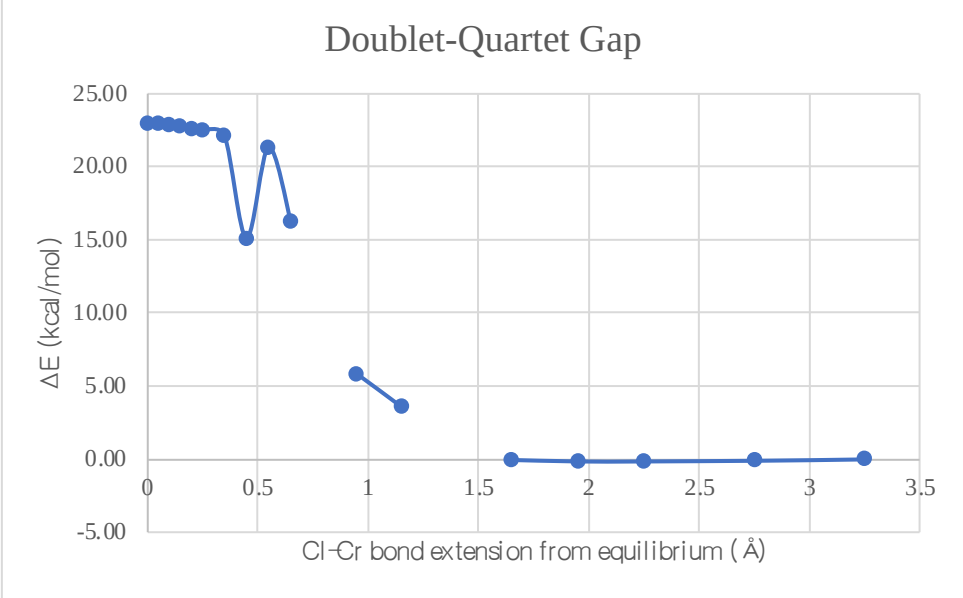

Figure 7.12 - Doublet-quartet gap of Cl-CrO_2 with varying Cl-Cr distance

The CrO_2 system is qualitatively similar to the VO_2 system when considering the effect of a Cl ligand. As the Cr-Cl distance decreases in the doublet Cl-CrO_2 system, the two bond lengths remain equal. They start at a value of 1.586 Å at large Cl-Cr distance, then contract to 1.557 Å before extending again to 1.561 Å. The triplet system exhibits different behavior with the dissociation of Cl. Upon introduction of Cl to the triplet CrO_2 system, one bond extends to 1.794 Å and the other contracts to 1.531 Å, with both bond lengths beginning with a value of 1.586 Å at large Cl-Cr distance. The doublet-quartet gap of the system has a value of 23.0 kcal/mol when considering the equilibrium structures. This value decreases slightly to 22.1 kcal/mol with the increase of the Cl-V distance before discontinuities appear. The curve becomes continuous again at a Cl-Cr bond length extension of 1.65 Å from equilibrium, and further extension results in the gap maintaining a near-zero value. Over the Cl-Cr extension range, the doublet-quartet gap ranges about 23 kcal/mol.

TiO_2, VO_2, and CrO_2 all have states in which ligation with Cl causes a sharp change in bond length but smooth changes in the potential energy curve. For Ti, the lower multiplicity has this character, but for V and Cr, the higher multiplicity has that character. The sharp convergence of the energetic gaps of these systems is due to spin interactions having a negligible effect on the energy of the system at larger distances. Unlike the NH_3 ligand, the Cl ligand has a much more pronounced effect on the bond lengths of the metal dioxides. This suggests that the Cl ligand may be able to stabilize the mechanisms of C-H bond activation that rely on the presence of metal-oxyl character.

Chapter 8 : Reactivity of MO_2 with CH_4

Introduction

Analysis of the reactivity of the metal dioxide systems with methane in the following section can be made clear with the lowest-energy electron configurations of each multiplicity in mind. These are the configurations that will determine the possible transition states and their geometries.

The lowest-energy singlet of TiO_2 has occupied valence orbitals of σ and π character, all three of which are polarized toward one oxygen atom of the metal. The lowest-energy triplet has doubly occupied σ and π orbital off the plane of the dioxide and singly occupied π orbital on the plane and δ_+ orbital with its density lying outside, above, and below the TiO_2 angle.

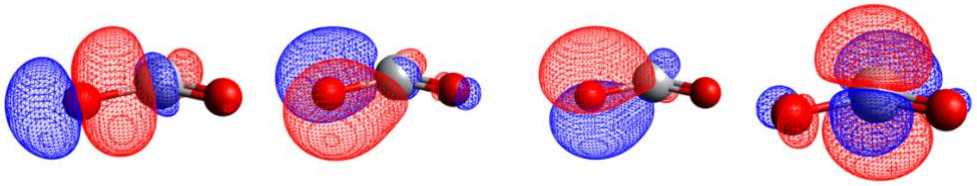

Figure 8.1 – Occupied orbitals for lowest singlet, triplet of TiO_2

From left to right: σ, π on plane, π off plane, δ_+ orbitals

The lowest-energy doublet of VO_2 has identical electron configuration to that of the lowest-energy singlet of TiO_2 save for the addition of an electron into the δ_+ orbital. The lowest-

energy quartet has identical electron configuration to that of the lowest-energy triplet of TiO_2 save for the addition of an electron into the δ_- orbital.

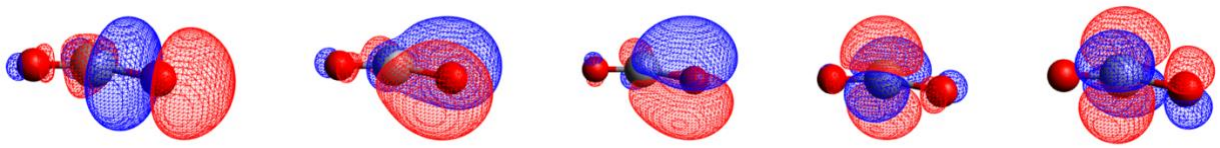

Figure 8.2 – Occupied orbitals for lowest doublet, quartet of VO_2

From left to right: σ, π on plane, π off plane, δ_+, δ_- orbitals

The lowest-energy triplet of CrO_2 has identical electron configuration to that of the lowest-energy doublet of VO_2 save for the addition of an electron into the δ_- orbital. The lowest-energy singlet has doubly occupied σ, π, and δ_+ orbitals. The lowest-energy quintet has doubly occupied σ and π on the plane orbitals and singly occupied δ_+, δ_-, π and π^* off the plane orbitals. CrO_2 differs from the other dioxides in the orientation of the singly occupied π orbital at high multiplicity; the orbital has density above and below the plane of the metal dioxide rather than on the plane.

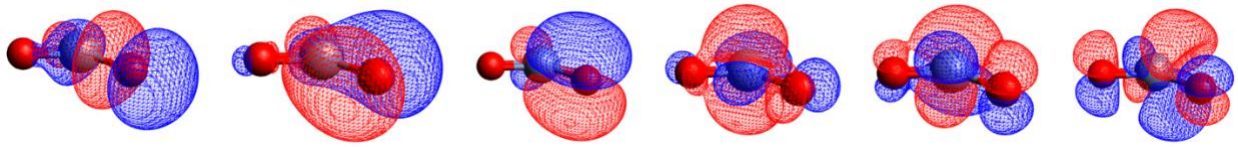

Figure 8.3 – Occupied orbitals for lowest triplet, singlet, quintet of CrO_2

From left to right: σ, π on plane, π off plane, δ_+, δ_-, π^* off plane orbitals

It has already been shown that transition metal oxide systems with primarily metal-oxyl character have much lower barriers to activating the C-H bond of methane, and those findings are consistent with the following data. The systems that exhibit metal-oxyl character are the lowest-energy triplet of TiO_2, quartet of VO_2, and quintet of CrO_2.

Three types of mechanisms have been elucidated for the transition metal monoxide systems.[17,18] One involves the concerted movement of two electrons, one is a radical mechanism, and the last is a proton-coupled electron transfer reaction[8]. The placement of all paths examined into these three categories has not been examined since orbital population analyses would be required, and that is outside the scope of this work. However, this work does confirm the presence of depressed activation energies in paths that include a metal-oxyl species, indicative of the path following a radical mechanism.

The transition states can be grouped into four categories based on the orientation of methane's approach to one of the oxygens of the MO_2 system. The following symbolism is used to describe these orientations: e – methane approaches exterior to the MO_2 angle, i – methane approaches interior to the MO_2 angle, l – methane approaches one of the oxygen atoms head-on, with the C, H, O, and M atoms colinear, and p – methane approaches at an angle not parallel to the plane of MO_2.

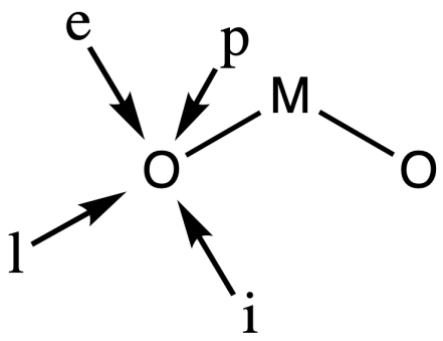

Figure 8.4 – Possible approaches of methane to the MO_2 system

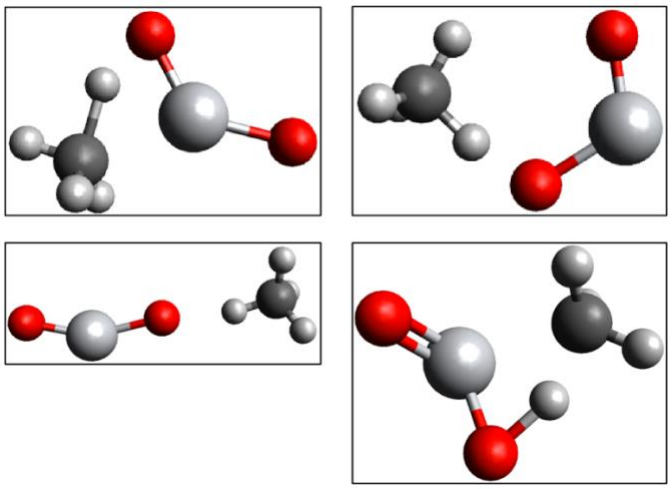

Figure 8.5 – Examples of approach types using transition states of TiO_2

Top left: e-type triplet transition state, top right: i-type triplet transition state,

bottom left: l-type triplet transition state, bottom right: p-type singlet transition state

Given the spatial orientation of the singly occupied orbitals of the highest-multiplicity systems considered in this study, predictions can be made about which transition state geometries will be most preferred by these systems and give the lowest activation energies. The i-type and e-type transition state geometries allow for higher orbital overlap between the soon-to-be-activated

C-H bond and the singly occupied π orbital of each system, with CrO_2 being the exception, allowing p-type transition state geometries to be low in energy as well.

Some reaction paths will be seen to end in a product interacting complex (PIC) that has a metal-carbon (M-C) bond. Those that do are much more likely to continue on a route that leads to the formation of methanol, with the oxygen of the hydroxyl moiety present in the PIC attacking the carbon of the methyl moiety. This path would follow first-order kinetics. Paths that end in PICs with no M-C bond involve the creation of a free methyl group, and further reactions that would lead to methanol would obey second-order kinetics. Since this is the first reaction in a series that leads to the creation of methanol, thermodynamics of the system will not be considered.

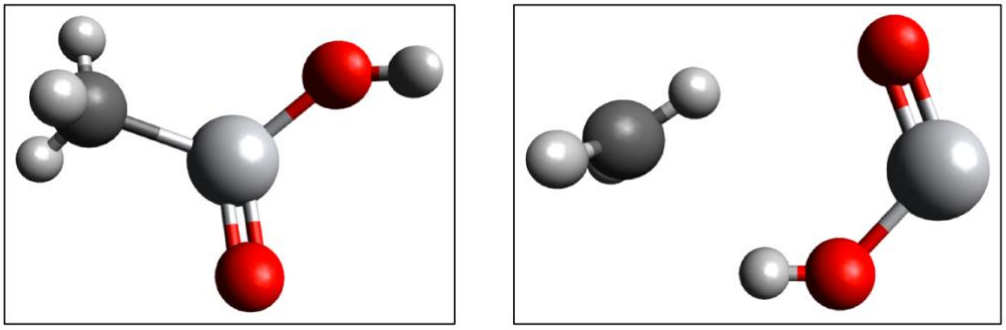

Figure 8.6 – Examples of PICs with and without a M-C bond

Left: PIC of path containing singlet p-type transition state of TiO_2, Right: PIC of path containing triplet i-type transition state of TiO_2

The column labeled ISR contains, for this system, the energies of infinitely separated reactants methane and either MO_2, H_3N-MO_2, or Cl-MO_2. These were calculated by setting to

zero the lowest-energy system of all multiplicities considered. The RIC column contains the energies of the interacting complex of these reactants, the TS column contains the energies of the transition states, and the PIC column contains the energies of the interacting complex of the products. The ISR energies were computed by running separate calculations for the MO_2 system in question and methane, and these values were then added for the ISR value. The highlighted entries matching in color in the following tables correspond to identical or near-identical structures.

MO_2

Metal dioxide	Orientation	Multiplicity	Sum of electronic and thermal free energies (kcal/mol)				E_a (kcal/mol)	M-C bond in PIC?
			ISR	RIC	TS	PIC		
TiO_2	i	3	46.84	52.04	57.08	34.77	5.04	
	e	3	46.84	43.81	59.02	34.76	15.21	
	p	1	0.00	-2.23	17.08	-23.23	19.31	Y
	e	3	46.84	43.79	66.00	31.12	22.21	Y
	l	1	0.00	4.55	50.16	35.34	45.61	
VO_2	e	4	30.81	27.42	39.97	5.14	12.55	Y
	p	2	0.00	-6.73	14.08	-25.25	20.80	Y
	e	4	30.81	27.42	50.69	21.96	23.27	Y
	i	2	0.00	4.90	37.65	14.78	32.76	
	p	2	0.00	-6.80	36.84	14.79	43.64	
CrO_2	i	5	37.61	42.47	45.20	19.06	2.73	
	e	5	37.61	41.64	47.69	19.11	6.05	
	e	5	37.61	43.52	61.33	20.74	17.80	Y
	e	3	0.00	-5.78	14.27	-23.99	20.05	Y
	p	1	23.87	16.52	39.21	-0.87	22.68	Y
	i	3	0.00	3.61	37.37	19.46	33.77	
	i	1	23.87	24.40	59.63		35.23	

Table 8.1 – Energetics of C-H bond activation paths by MO_2 | M=Ti, V, Cr

Five distinct transition states were found for the bare TiO_2 system. Two transition states were found for singlet TiO_2, and three were found for triplet TiO_2. The low-multiplicity system has transition states of p- and l-type, and the high-multiplicity system has transition states of e- and i-type. The triplet mechanisms of C-H bond activation are relatively inaccessible due to the 46.8 kcal/mol barrier. The two e-type transition states found share reactant interacting complexes (RICs), but not product interacting complexes (PICs), and the lowest-barrier i-type and e-type transition states share products. These lowest-barrier to activation paths do not result in the creation of a M-C bond. The only l-type transition state found also does not result in a PIC with a M-C bond. The PICs that do have a M-C bond are the result of a singlet p-type and triplet e-type transition state, both of which have comparable activation barriers at 19.3 and 22.2 kcal/mol, respectively.

Five transition states were also found for the bare VO_2 system. Three transition states were found for doublet VO_2, and two were found for quartet VO_2. The low-multiplicity system has transition states of the p- and i- type, and the high-multiplicity system has only e-type transition states. Similar to the TiO_2 system, the quartet (higher multiplicity) mechanisms of C-H bond activation are relatively inaccessible due to the 30.8 kcal/mol barrier. The two e-type transition states share RICs but not PICs, and the two p-type transition states do as well. The highest-activation barrier mechanisms share PICs, but not RICs. The three lowest-barrier to activation paths found do result in the creation of a M-C bond in their PICs, and have either an e- or p-type transition state. Again, having the p-type geometry of the transition state does not guarantee the presence of a M-C bond in the PIC, evidenced by the path with a doublet p-type transition state. The paths that do result in a M-C bond have disparate activation barriers ranging

from 12.6 to 23.3 kcal/mol, and those that do not are also far apart in energy at 32.8 and 43.6 kcal/mol.

Seven transition states were found for the bare CrO_2 system. There were two, two, and three transition states for the singlet, triplet, and quintet systems, respectively. The lowest multiplicity system had transition states of the i- and p-type, and the higher multiplicity systems were of the e- and i-types. Again, the highest multiplicity (and lower activation energy) paths are less accessible due to the 37.6 kcal/mol barrier, but they come with the lowest activation energies for C-H bond activation. The two paths with the lowest activation energies and the triplet path with the i-type transition state all share PIC geometries. Only one path of each multiplicity results in the creation of a M-C bond, and result from either of e- or p-type transition states. These paths have relatively similar activation energies ranging from 17.8 to 22.7 kcal/mol, and the paths not resulting in this connectivity have an activation energy either 11 kcal/mol higher or lower than that range.

These metal dioxides are capable of a wide variety of C-H bond activation paths. The highest multiplicity paths of each system have high barriers, but have the lowest activation energies associated with them, which is consistent with prior work of the Miliordos group. For the bare MO_2 system, the presence of an M-C bond in the PICs requires either an e- or p-type transition state, but the geometry of the transition state does not predict the presence of a M-C bond, as there is a p-type transition state of the VO_2 system that results in a free methyl product. The activation energies of the paths with PICs containing M-C bonds fall in the middle of the range of activation energies found across all paths examined.

H_3N-MO_2

System	Orientation	Multiplicity	Sum of electronic and thermal free energies (kcal/mol)				E_a (kcal/mol)	M-C bond in PIC?
			ISR	RIC	TS	PIC		
H_3N-TiO_2	i	3	47.34	52.43	58.19	35.38	5.77	
	p	1	0.00	-0.95	15.90	-22.95	16.85	Y
H_3N-VO_2	i	4	35.28	40.12	44.70	21.48	4.58	
	e	4	35.28	41.47	47.65	21.45	6.17	
	p	2	0.00	-1.28	18.21	-17.57	19.48	Y
H_3N-CrO_2	p	5	72.58910	55.50702	60.98393	37.38956	5.48	
	p	1	21.95093	27.84450	47.98130	13.81840	20.14	Y
	p	1	21.95093	27.84889	68.04718	13.82656	40.20	Y

Table 8.2 – Energetics of C-H bond activation paths by H_3N-MO_2 | M=Ti, V, Cr

Two paths were found for the H_3N-TiO_2 system, one of each multiplicity. The singlet path was found to have a higher activation energy at 16.9 kcal/mol, and the triplet path was found to have a high barrier at 47.3 kcal/mol. The singlet system resulted in the creation of an M-C bond, and the triplet system did not.

Three paths were found for the H_3N-VO_2 system. The lower activation energy systems were quartets with transition states of the i- and e-type, and the highest was the doublet system with a p-type transition state. The only path found with a RIC of lower energy than the ISR was the doublet system, and this was also the only path that gave rise to a M-C bond. The quartet systems were also found to share a PIC.

Three paths were found for the H_3N-CrO_2 system. One quintet path was found along with two singlet paths, but no triplet paths were found. All paths found had p-type transition states. The singlet paths share both a RIC and a PIC with a M-C bond, but go through two different

transition states, both of p-type. The highest multiplicity path was again found to have a lower activation energy than that of the lower-multiplicity systems.

Significantly less paths were found for the ammonia-ligated systems than for the bare systems, and the proportion of paths with M-C bonds is less than that of the bare systems.

Cl-MO_2

System	Orientation	Multiplicity	Sum of electronic and thermal free energies (kcal/mol)				E_a (kcal/mol)	M-C bond in PIC?
			ISR	RIC	TS	PIC		
Cl-TiO_2	e	4	62.15	67.73	69.25	43.20	1.51	
	i	4	62.15	66.02	68.87	44.54	2.85	
	i	2	0.00	6.66	10.17	-10.77	3.50	
	i	2	0.00	5.99	10.17	-10.79	4.18	
	e	2	0.00	-1.36	11.63	-8.69	12.99	
	p	2	0.00	-1.33	26.71	-1.83	28.04	Y
Cl-VO_2	i	3	34.49	39.85	42.68	21.84	2.84	
	e	3	34.49	39.06	44.19	23.05	5.13	
	p	3	34.49	39.05	50.12	15.28	11.07	Y
	p	1	0.00	-4.90	18.80	-14.66	23.70	Y
	l	1	0.00	5.63	38.07	21.43	32.45	
	i	1	0.00	-4.92	41.98	21.21	46.90	
Cl-CrO_2	e	4	22.16	27.99	31.78	9.98	3.79	
	i	4	22.16	26.58	30.45	7.85	3.87	
	p	2	0.00	3.59	23.48	-12.37	19.89	Y
	p	2	0.00	3.60	24.05	8.55	20.45	
	p	2	0.00	3.60	44.09	8.23	40.50	

Table 8.3 – Energetics of C-H bond activation paths by Cl-MO_2 | M=Ti, V, Cr

Six paths were found for the Cl-TiO_2 system. Two quartet paths were found, and the remainder were doublets. The two doublet paths lowest in activation energy share transition states and PICs, but have different RICs. Only one path resulted in a PIC with a M-C bond, and that path that had a p-type transition state.

Six paths were also found for the Cl-VO_2 system, evenly split between singlets and triplets. The triplet paths with the e- and p-type transition states shared RICs, and the singlet paths with the i- and l-type transition states share PICs. One path of each multiplicity has a PIC with a M-C bond, both of which have p-type transition states.

Six paths were found again for the Cl-CrO_2 system, evenly split between doublets and quartets. The quartet path with i-type transition state and the doublet path with p-type transition state share a PIC, and all doublet paths share the same RIC. Only one path has a PIC with a M-C bond, and follows from a doublet p-type transition state.

Ligand effects on MO_2 reactivity

From the collection of found structures, analogous paths can be identified by grouping paths with identical transition state type and similar ISR energy. The activation energies of the paths can then be compared. However, not all types of transition states have partners.

Ligand	Orientation	Multiplicity	Sum of electronic and thermal free energies (kcal/mol)				E_a (kcal/mol)	M-C bond in PIC?
			ISR	RIC	TS	PIC		
none	i	3	46.84	52.04	57.08	34.77	5.04	
NH_3	i	3	47.34	52.43	58.19	35.38	5.77	
Cl	i	4	62.15	66.02	68.87	44.54	2.85	
none	e	3	46.84	43.81	59.02	34.76	15.21	
Cl	e	4	62.15	67.73	69.25	43.20	1.51	
none	e	3	46.84	43.79	66.00	31.12	22.21	Y
Cl	i	2	0.00	6.66	10.17	-10.77	3.50	
Cl	i	2	0.00	5.99	10.17	-10.79	4.18	
Cl	e	2	0.00	-1.36	11.63	-8.69	12.99	
none	l	1	0.00	4.55	50.16	35.34	45.61	
none	p	1	0.00	-2.23	17.08	-23.23	19.31	Y
NH_3	p	1	0.00	-0.95	15.90	-22.95	16.85	Y
Cl	p	2	0.00	-1.33	26.71	-1.83	28.04	Y

Table 8.4 – Ligand effects on the energetics of C-H bond activation paths by TiO_2

For the TiO_2 system, high-multiplicity i-type transition states were found for the bare metal, Cl-ligated, and NH_3-ligated systems. The addition of the Cl ligand decreased the activation energy by just over 2 kcal/mol, and adding NH_3 had the effect of increasing the barrier height by less than 1 kcal/mol. The next type of path for which there were comparable systems is the high-multiplicity e-type transition state paths, in which the addition of one Cl ligand depressed the barrier height by almost 14 kcal/mol. The last path type of which transition states were found for all three ligation types is the low-multiplicity p-type transition state paths, all of which resulted in M-C bond formation in the PICs. The addition of the NH_3 ligand decreased the barrier height by 2.5 kcal/mol, and the addition of the Cl ligand increased the barrier height by 8.7 kcal/mol.

Ligand	Orientation	Multiplicity	Sum of electronic and thermal free energies (kcal/mol)				E_a (kcal/mol)	M-C bond in PIC?
			ISR	RIC	TS	PIC		
NH_3	i	4	35.28	40.12	44.70	21.48	4.58	
Cl	i	3	34.49	39.85	42.68	21.84	2.84	
none	e	4	30.81	27.42	39.97	5.14	12.55	Y
none	e	4	30.81	27.42	50.69	21.96	23.27	Y
NH_3	e	4	35.28	41.47	47.65	21.45	6.17	
Cl	e	3	34.49	39.06	44.19	23.05	5.13	
Cl	p	3	34.49	39.05	50.12	15.28	11.07	Y
none	i	2	0.00	4.90	37.65	14.78	32.76	
Cl	i	1	0.00	-4.92	41.98	21.21	46.90	
Cl	l	1	0.00	5.63	38.07	21.43	32.45	
none	p	2	0.00	-6.73	14.08	-25.25	20.80	Y
NH_3	p	2	0.00	-1.28	18.21	-17.57	19.48	Y
Cl	p	1	0.00	-4.90	18.80	-14.66	23.70	Y
none	p	2	0.00	-6.80	36.84	14.79	43.64	

Table 8.5 – Ligand effects on the energetics of C-H bond activation paths by VO_2

The VO_2 system and its ligated counterparts offered three pairs and one triple from which conclusions could be drawn. The high-multiplicity paths with analogous i-type transition states were only found for the H_3N-VO_2 and Cl-VO_2 systems, and the activation energies differ by 1 kcal/mol. The low-multiplicity paths with analogous i-type transition states were only found for the bare VO_2 and Cl-VO_2 systems, and the addition of the Cl ligand raises the barrier height by just over 14 kcal/mol. The only path for which all three ligated systems were found is the low-multiplicity path with a p-type transition state, and these paths all resulted in M-C bond formation in the PICs as well. For this path, addition of NH_3 lowered the barrier height by 1.3 kcal/mol, and addition of Cl raised the barrier height by 2.9 kcal/mol.

Ligand	Orientation	Multiplicity	Sum of electronic and thermal free energies (kcal/mol)				E_a (kcal/mol)	M-C bond in PIC?
			ISR	RIC	TS	PIC		
NH_3	p	5	72.59	55.51	60.98	37.39	5.48	
none	i	5	37.61	42.47	45.20	19.06	2.73	
none	e	5	37.61	41.64	47.69	19.11	6.05	
none	e	5	37.61	43.52	61.33	20.74	17.80	Y
none	i	1	23.87	24.40	59.63		35.23	
Cl	i	4	22.16	27.96	30.43	7.28	2.47	
Cl	i	4	22.16	26.58	30.45	7.85	3.87	
Cl	e	4	22.16	27.99	31.78	9.98	3.79	
none	p	1	23.87	16.52	39.21	-0.87	22.68	Y
NH_3	p	1	21.95	27.84	47.98	13.82	20.14	Y
NH_3	p	1	21.95	27.85	68.05	13.83	40.20	Y
none	i	3	0.00	3.61	37.37	19.46	33.77	
none	e	3	0.00	-5.78	14.27	-23.99	20.05	Y
Cl	p	2	0.00	3.59	23.48	-12.37	19.89	Y
Cl	p	2	0.00	3.60	24.05	8.55	20.45	
Cl	p	2	0.00	3.60	44.09	8.23	40.50	

Table 8.6 – Ligand effects on the energetics of C-H bond activation paths by CrO_2

The CrO_2 system has far less to offer in terms of available data for comparison of ligand effects on activation barriers, having only two analogous paths. For the CrO_2 system, the distinction of high and low multiplicity was less helpful in grouping analogous paths. Recall that the quintet CrO_2 system is the first to exhibit metal-oxyl character, and the lower-multiplicity systems have significant metal-oxo character; the numerical value of the system's multiplicity has no direct correlation with emergence of metal-oxyl character for this transition metal dioxide.

The path of singlet bare CrO_2 and quartet Cl-CrO_2, both having an i-type transition state, were found to be analogous, with the barrier height dropping over 30 kcal/mol with the addition of the Cl ligand. The singlet paths with analogous p-type transition states were only found for the bare and NH_3-ligated systems, and the addition of the ammonia ligand decreased the barrier height by just over 2 kcal/mol.

One important caveat to be made is that although these groupings can be made, conclusions drawn from these groupings should be taken lightly; systems with analogous transition states do not consistently converge to analogous reactant structures in the case of the systems involving V and Cr. As such, these systems are not strictly, but loosely analogous.

Future directions

Further study of the total reaction path and conversion to the final product of methane will be crucial to drawing more significant conclusions, considering the thermodynamics of the reaction landscapes rather than the kinetics of these geometrically dissimilar reactant and transition state pairs. Further work should also be done to assess the MN15 functional's performance in terms of size-extensivity to determine the reliability of the values resulting from simple addition of infinitely separated reactants, as RIC values are not consistently lower in energy than the ISR values of the same system. In addition to this, a control study of sorts should be done with an active space that includes the 2s orbital of the other oxygen atom in order to confirm the equivalent bond lengths reported by DFT at the MRCI level of theory. One other avenue that could be explored would be the replacement of the oxo ligand of the TiO_2 system with two Cl ligands, which should behave in much the same manner save for the steric effects of

adding another atom into the system. Finally, the mechanisms of all paths should be elucidated, and categorization of these mechanisms into the aforementioned three types (concerted, radical, proton-coupled electron transfer) should be done.

References

(1) Pawłowski, F. CC Energy and Amplitude Equations. *Special Topics in Physical Chemistry II*, 2021.

(2) Taylor, P. R.; Olsen, J. Multiconfigurational and multireference methods. *The Multiconfigurational Approach*, 2019.

(3) Density functional (DFT) methods. https://gaussian.com/dft/ (accessed Dec 25, 2021).

(4) Zhang, I. Y.; Wu, J.; Xu, X. *Chemical Communications*, **2010**, *46* (18), 3057–3070.

(5) Yu, H. S.; He, X.; Li, S. L.; Truhlar, D. G. *Chemical Science*, **2016**, *7* (8), 5032–5051.

(6) Miliordos, E.; Mavridis, A. *The Journal of Physical Chemistry A*, **2010**, *114* (33), 8536–8572.

(7) Khan, S. N.; Miliordos, E. *J. Phys. Chem. A*, **2019**, *123* (26), 5590–5599.

(8) Sader, S.; Miliordos, E. *J. Phys. Chem. A*, **2021**, *125* (11), 2364–2373.

(9) Kirkland, J. K.; Khan, S. N.; Casale, B.; Miliordos, E.; Vogiatzis, K. D. *Phys. Chem. Chem. Phys.*, **2018**, *20* (45)**,** 28786-28795.

(10) Liu, G.; Zhu, Z.; Ciborowski, S. M.; Ariyarathna, I. R.; Miliordos, E.; Bowen, K. H.; *Angew. Chem. Int. Ed.*, **2019**, *58*, 7773.

(11) Latimer, A. A.; Kakekhani, A.; Kulkarni, A. R.; Nørskov, J. K. *ACS Catal.*, **2018**, *8* (8), 6894–6907.

(12) Najafian, A.; Cundari, T. R. *Inorg. Chem.*, **2017**, *56* (20), 12282–12290.

(13) Claveau, E. E.; Miliordos, E. *Phys. Chem. Chem. Phys*., **2021**, *23* (37), 21172-21182.

(14) Ariyarathna, I. R.; Miliordos, E. *Phys. Chem. Chem. Phys*., **2021**, *23* (2), 1437-1442.

(15) Claveau, E. E.; Miliordos, E. *Phys. Chem. Chem. Phys*., **2019**, *21* (48), 26324-26332.

(16) Jackson, B. A.; Miliordos, E. *Phys. Chem. Chem. Phys*., **2020**, *22* (12), 6606-6618.

(17) Schwarz, H. *Angewandte Chemie International Edition*, **2011**, *50* (43), 10096–10115.

(18) Carsch, K. M.; Cundari, T. R. *Computational and Theoretical Chemistry*, **2012**, *980*, 133-137.

(19) Raghavachari, K.; Trucks, G. W.; Pople, J. A.; Head-Gordon, M. *Chem. Phys. Lett*., **1989**, *157*, 479.

(20) Watts, J. D.; Bartlett, R. J. *J. Chem. Phys*., **1993**, *98*, 8718.

(21) Knowles, P. J.; Hampel, C.; Werner, H. J. *J. Chem. Phys*., **1993**, *99*, 5219; ibid. **2000**, *112*, 3106E.

(22) Helgaker, T. J.; Olsen, J. *Molecular electronic-structure theory*, 1st ed.; Wiley, 2014.

(23) Dunning, T. H. *J. Chem. Phys.*, **1989**, *90*, 1007.

(24) Balabanov, N. B.; Peterson, K. A. *J. Chem. Phys.*, **2005**, *123*, 064107.

(25) Gaussian 16, Revision C.01, Frisch, M. J.; Trucks, G. W.; Schlegel, H. B.; Scuseria, G. E.; Robb, M. A.; Cheeseman, J. R.; Scalmani, G.; Barone, V.; Petersson, G. A.; Nakatsuji, H.; Li, X.; Caricato, M.; Marenich, A. V.; Bloino, J.; Janesko, B. G.; Gomperts, R.; Mennucci, B.; Hratchian, H. P.; Ortiz, J. V.; Izmaylov, A. F.; Sonnenberg, J. L.; Williams-Young, D.; Ding, F.; Lipparini, F.; Egidi, F.; Goings, J.; Peng, B.; Petrone, A.; Henderson, T.; Ranasinghe, D.; Zakrzewski, V. G.; Gao, J.; Rega, N.; Zheng, G.; Liang, W.; Hada, M.; Ehara, M.; Toyota, K.; Fukuda, R.; Hasegawa, J.; Ishida, M.; Nakajima, T.; Honda, Y.; Kitao, O.; Nakai, H.; Vreven, T.; Throssell, K.; Montgomery, J. A., Jr.; Peralta, J. E.;

Ogliaro, F.; Bearpark, M. J.; Heyd, J. J.; Brothers, E. N.; Kudin, K. N.; Staroverov, V. N.; Keith, T. A.; Kobayashi, R.; Normand, J.; Raghavachari, K.; Rendell, A. P.; Burant, J. C.; Iyengar, S. S.; Tomasi, J.; Cossi, M.; Millam, J. M.; Klene, M.; Adamo, C.; Cammi, R.; Ochterski, J. W.; Martin, R. L.; Morokuma, K.; Farkas, O.; Foresman, J. B.; Fox, D. J. Gaussian, Inc., Wallingford CT, 2016.

(26) H.-J. Werner, P. J. Knowles, G. Knizia, F. R. Manby and M. Schütz, *WIREs Comput Mol Sci*, **2012**, *2*, 242–253.

(27) Hans-Joachim Werner, Peter J. Knowles, Frederick R. Manby, Joshua A. Black, Klaus Doll, Andreas Heßelmann, Daniel Kats, Andreas Köhn, Tatiana Korona, David A. Kreplin, Qianli Ma, Thomas F. Miller, III, Alexander Mitrushchenkov, Kirk A. Peterson, Iakov Polyak, Guntram Rauhut, and Marat Sibaev J. Chem. Phys., **2020**, *152*, 144107.

(28) MOLPRO, 15, a package of ab initio programs, H.-J. Werner, P. J. Knowles, G. Knizia, F. R. Manby, M. Schütz, P. Celani, W. Györffy, D. Kats, T. Korona, R. Lindh, A. Mitrushenkov, G. Rauhut, K. R. Shamasundar, T. B. Adler, R. D. Amos, S. J. Bennie, A. Bernhardsson, A. Berning, D. L. Cooper, M. J. O. Deegan, A. J. Dobbyn, F. Eckert, E. Goll, C. Hampel, A. Hesselmann, G. Hetzer, T. Hrenar, G. Jansen, C. Köppl, S. J. R. Lee, Y. Liu, A. W. Lloyd, Q. Ma, R. A. Mata, A. J. May, S. J. McNicholas, W. Meyer, T. F. Miller III, M. E. Mura, A. Nicklass, D. P. O'Neill, P. Palmieri, D. Peng, T. Petrenko, K. Pflüger, R. Pitzer, M. Reiher, T. Shiozaki, H. Stoll, A. J. Stone, R. Tarroni, T. Thorsteinsson, M. Wang, and M. Welborn.

(29) Selected Tables of Atomic Spectra, Atomic Energy Levels and Multiplet Tables – O I, C. E. Moore, in Nat. Stand. Ref. Data Ser., NSRDS-NBS 3 (Sect. 7), 33 pp. (Nat. Bur. Stand., U.S., 1976)

Appendix 1 – DFT Optimal geometries (Cartesian coordinates in Å)

Table A1 – TiO_2 monomeric structures

System	Coordinates
1et TiO_2	Ti 0.000000 0.376417 0.000000 O 1.357703 -0.517497 -0.000000 O -1.357703 -0.517649 -0.000000
3et TiO_2	Ti 0.000000 0.413375 -0.000000 O 1.410762 -0.794491 0.000000 O -1.410762 -0.342290 0.000000
1et H_3N-TiO_2	Ti 0.310436 0.000013 0.357186 O 0.790380 -1.378720 -0.394994 O 0.789991 1.378882 -0.394984 N -1.853323 -0.000174 -0.098069 H -2.394262 0.828405 0.129175 H -1.711292 0.000661 -1.108858 H -2.393748 -0.829436 0.127908
3et H_3N-TiO_2	Ti 0.203085 -0.008942 -0.000049 O 1.884008 -0.880464 0.000052 O 0.134975 1.608972 0.000042 N -1.952235 -0.562756 0.000025 H -2.331901 -0.086142 -0.817474 H -2.290390 -1.519924 0.000149 H -2.331812 -0.085974 0.817472
2et Cl-TiO_2	Ti 0.402872 0.036963 0.000423 O 1.645807 -1.297614 -0.000395 O 1.137708 1.443195 -0.000413 Cl -1.831254 -0.116342 -0.000167
4et Cl-TiO_2	Ti 0.420937 -0.000009 -0.000060 O 1.308537 -1.620861 0.000059 O 1.308652 1.620819 0.000059 Cl -1.776360 0.000032 0.000022

Table A2 – VO_2 monomeric structures

System	Coordinates
2et VO_2	V 0.000000 0.341231 0.000000 O 1.362552 -0.490540 -0.000000 O -1.362552 -0.490498 -0.000000
4et VO_2	V 0.000000 0.215338 0.000000 O 1.582105 -0.827691 -0.000000 O -1.582105 0.208596 0.000000
2et H_3N-VO_2	V 0.270233 0.000010 0.274774 O 0.819789 1.396438 -0.307476 O 0.820234 -1.396234 -0.307492 N -1.833855 -0.000185 -0.098767 H -1.985520 0.823464 -0.676955 H -1.985919 -0.824541 -0.675836 H -2.527110 0.000504 0.644097
4et H_3N-VO_2	V -0.225955 0.113871 -0.000027 O -1.676274 -1.084869 0.000028 O -0.014177 1.691951 0.000031 N 1.765303 -0.724122 0.000011 H 2.017310 -1.265716 -0.821934 H 2.328846 0.124363 -0.000103 H 2.017286 -1.265486 0.822113
1et Cl-VO_2	V 0.420300 0.000001 -0.160968 O 1.245393 1.288088 0.167458 O 1.245375 -1.288098 0.167456 Cl -1.740767 0.000003 0.060173
3et Cl-VO_2	V 0.390955 -0.045090 0.000055 O 1.541208 1.322577 -0.000054 O 1.080713 -1.438577 -0.000058 Cl -1.762784 0.115592 -0.000022

Table A3 – CrO_2 monomeric structures

System	Coordinates
1et CrO_2	Cr 0.000000 0.293066 0.000000 O 1.391635 -0.439593 -0.000000 O -1.391635 -0.439605 -0.000000
3et CrO_2	Cr 0.000000 0.241093 -0.000000 O 1.467099 -0.361649 0.000000 O -1.467099 -0.361630 0.000000
5et CrO_2	Cr 0.000000 0.234036 -0.000000 O 1.551176 0.024013 -0.000000 O -1.551176 -0.726122 0.000000
1et H_3N-CrO_2	Cr 0.219706 -0.000053 0.000001 O 0.867123 1.446714 -0.000004 O 0.935765 -1.413440 -0.000005 N -1.860906 -0.028348 -0.000008 H -2.203255 0.929685 0.002239 H -2.233318 -0.496173 -0.822621 H -2.233127 -0.500004 0.820502
3et H_3N-CrO_2	Cr 0.242546 0.001558 0.000060 O 0.820036 1.488103 -0.000073 O 0.905168 -1.448171 -0.000070 N -1.853778 -0.036083 -0.000037 H -2.204245 0.918658 0.000948 H -2.221040 -0.510654 -0.820661 H -2.220994 -0.512282 0.819667
5et H_3N-CrO_2	Cr 0.186253 0.082557 -0.000006 O 0.154729 1.686218 0.000007 O 1.659370 -1.107593 0.000006 N -1.793099 -0.630763 0.000003 H -2.280813 -0.275571 -0.818812 H -1.869362 -1.644637 0.000460 H -2.281006 -0.274820 0.818377
2et Cl-CrO_2	Cr 0.397265 0.000001 0.000411 O 1.229392 -1.321239 -0.000442 O 1.229395 1.321235 -0.000442 Cl -1.717921 0.000000 -0.000164
4et Cl-CrO_2	Cr 0.000000 0.425090 -0.000000 O 1.716910 0.943730 0.000000 O -1.189162 1.389312 -0.000000

	Cl -0.248352 -1.698029 0.000000
6et Cl-CrO_2	Cr -0.370937 0.003467 -0.000076 O -1.193445 -1.597755 0.000077 O -1.432304 1.471238 0.000081 Cl 1.759323 0.054643 0.000033

Table A4 – Methane, NH_3

System	Coordinates
1et CH_4	C 0.000000 0.000002 -0.000001 H -0.791012 0.574482 -0.475474 H -0.340991 -0.352127 0.970328 H 0.876698 0.629422 0.130518 H 0.255302 -0.851787 -0.625367
1et NH_3	N -0.000082 0.000012 -0.111757 H 0.525458 0.782466 0.260701 H -0.940256 0.063513 0.260920 H 0.415375 -0.846064 0.260679

Table A5 – TiO_2 reaction paths in order of increasing E_a

System	Reactant Interacting Complex	Transition State	Product Interacting Complex
3et i-type	Ti 1.191942 -0.080106 0.000084 O 0.566558 1.394782 -0.000148 O -0.114462 -1.405157 -0.000153 C -2.984099 0.184759 0.000058 H -3.583398 0.380175 -0.886469 H -2.659788 -0.853879 -0.002675 H -3.580424 0.376420 0.889404 H -2.111296 0.834053 -0.000050	Ti -1.027457 -0.221987 -0.000001 O -0.798766 1.370162 0.000003 O 0.522648 -1.199866 0.000003 C 2.505580 0.375796 -0.000001 H 3.079339 0.202982 0.904431 H 1.644437 -0.462313 -0.000001 H 3.079094 0.203236 -0.904636 H 1.976655 1.322667 0.000199	Ti 1.103377 -0.078133 0.000072 O 0.537675 1.431305 0.000104 O -0.148502 -1.396089 -0.000128 C -2.914076 0.306307 -0.000139 H -3.388727 0.042838 -0.929547 H -1.112108 -1.387105 -0.000178 H -3.388036 0.043423 0.929787 H -2.014345 0.900191 -0.000619
3et e-type	Ti 0.201388 -0.013536 -0.002339 O 0.374777 -1.616790 0.002207 O 1.746030 1.068178 0.002444 C -2.127574 0.471118 0.000957 H -3.210613 0.517686 0.011749 H -1.751032 1.497902 -0.023644 H -1.843495 -0.097115 -0.901016 H -1.826410 -0.058504 0.921414	Ti 0.670283 -0.333429 -0.000030 O 2.185656 0.191919 0.000070 O -0.615772 1.019705 -0.000034 C -2.759065 -0.261765 0.000056 H -3.281465 0.022610 -0.905991 H -1.733527 0.480553 0.000036 H -2.458385 -1.306475 -0.004298 H -3.277529 0.016360 0.910289	Ti -1.103584 0.077952 -0.000119 O -0.537302 -1.431254 0.000193 O 0.148007 1.396298 0.000231 C 2.914685 -0.305820 -0.000129 H 2.015073 -0.899880 0.000406 H 1.111576 1.385482 0.000498 H 3.388380 -0.042572 -0.930086 H 3.390076 -0.043394 0.929192

1et p-type	Ti -0.298113 0.000013 0.302881 O -0.928223 1.367650 -0.330183 O -0.927609 -1.367944 -0.330146 C 2.128395 0.000173 -0.134213 H 3.146960 0.000787 -0.506451 H 2.181171 0.000479 0.959465 H 1.653708 -0.913443 -0.513978 H 1.652931 0.913206 -0.514516	Ti -0.338375 -0.004971 -0.354058 O 0.218265 -1.482447 0.296855 O -1.515607 0.720138 0.478702 C 1.748021 0.670905 0.135434 H 2.674343 0.232842 0.505666 H 1.976976 1.055479 -0.866912 H 1.500873 1.507821 0.787974 H 1.182669 -0.613737 0.345491	Ti 0.084649 -0.097416 -0.220496 O 1.447424 1.048389 0.126565 O 0.265186 -1.620411 0.226264 C -1.866378 0.590138 0.136199 H -2.024646 1.600597 -0.251917 H -2.627060 -0.075364 -0.280180 H -2.032551 0.621330 1.217613 H 2.319379 1.031934 0.525583
3et e-type	Ti 0.201262 0.013796 -0.000096 O 1.744992 -1.069215 0.000103 O 0.375493 1.616950 0.000093 C -2.127015 -0.470947 0.000059 H -1.749280 -1.497461 0.001500 H -1.834969 0.077047 -0.912223 H -1.835251 0.079510 0.910893 H -3.210049 -0.518809 0.000029	Ti 0.265836 -0.015435 0.070377 O 2.091204 -0.475536 -0.086370 O -0.522225 1.481324 -0.050000 C -1.801963 -0.818369 -0.041864 H -1.570698 -1.550544 -0.824388 H -1.411665 0.579541 -0.108461 H -1.777078 -1.326337 0.931325 H -2.829000 -0.499166 -0.204628	Ti 0.085201 -0.056398 0.023217 O 0.664697 -1.827030 -0.023736 O 1.224032 1.310964 -0.015632 C -1.957798 0.356324 -0.019368 H -2.411741 -0.453087 -0.604900 H 1.778489 2.089144 -0.047601 H -2.334763 0.281727 1.007821 H -2.269441 1.313557 -0.434944
1et l-type	Ti -1.220951 -0.382252 -0.000025 O -2.023511 1.030360 -0.000003 O 0.394451 -0.199863 0.000104 C 3.988101 0.176341 -0.000020 H 4.331472 0.707273 -0.885214 H 2.901554 0.131047 0.000954 H 4.333399 0.700704 0.888336 H 4.398363 -0.831493 -0.004220	Ti 0.985686 -0.388469 -0.000028 O 1.993290 0.874502 -0.000007 O -0.713559 -0.029343 0.000142 C -3.260764 0.180679 -0.000038 H -3.450535 0.779067 0.882683 H -1.832175 0.082348 -0.000009 H -3.460451 0.680830 -0.939858 H -3.615181 -0.841271 0.056937	Ti -1.096129 -0.073774 0.000035 O -0.521140 1.432166 -0.000064 O 0.141420 -1.406193 -0.000052 C 2.888510 0.305381 0.000029 H 2.012400 0.933130 -0.000163 H 1.105092 -1.396637 -0.000093 H 3.351893 0.023324 0.929758 H 3.352149 0.023139 -0.929517

Table A6 – VO_2 reaction paths in order of increasing E_a

System	Reactant Interacting Complex	Transition State	Product Interacting Complex
4et e-type	V 0.296135 0.089521 -0.012976 O 0.679283 1.627226 0.016358 O 1.135805 -1.590285 0.013772 C -2.123349 -0.235321 0.012766 H -2.418499 -0.306666 1.054491 H -1.507649 -1.105972 -0.261119 H -1.669338 0.752766 -0.181655 H -2.996221 -0.282704 -0.630897	V 0.464833 0.022358 0.000006 O 1.993727 -0.407088 -0.000009 O -0.884285 1.362667 -0.000013 C -1.958040 -0.853210 -0.000005 H -2.533844 -0.958177 -0.910722 H -1.643089 0.431940 0.000234 H -1.108603 -1.554556 -0.000668 H -2.532914 -0.958806 0.911224	V -0.173071 -0.232867 -0.000296 O 0.439461 -1.711492 0.000369 O -1.628915 0.856328 0.000018 C 1.761748 1.220984 0.000234 H 1.680871 1.757786 0.931146 H -2.530732 1.170163 0.001046 H 2.090301 0.183469 -0.000119 H 1.685329 1.759932 -0.929766
2et p-type	V -0.248090 0.000003 0.185167 O -0.955735 1.385498 -0.203910 O -0.955252 -1.385736 -0.203880	V 0.318439 0.036178 -0.291392 O -0.301191 1.490334 0.269584 O 1.526604 -0.717716 0.401897	V 0.080536 -0.102393 -0.180277 O 1.467068 0.958682 0.109101 O 0.095717 -1.620666 0.199984

	C 2.086155 0.000210 -0.092097	C -1.673932 -0.750908 0.104272	C -1.742179 0.699734 0.139211
	H 3.081746 -0.000289 -0.522269	H -2.519412 -0.447314 0.721766	H -2.374723 0.179124 0.852676
	H 2.183579 0.001536 0.996907	H -2.061834 -0.959820 -0.895949	H -1.689469 1.762760 0.373984
	H 1.606094 -0.920924 -0.458225	H -1.281147 -1.665793 0.550478	H -2.189968 0.584914 -0.864178
	H 1.605627 0.920239 -0.460348	H -1.221409 0.565346 0.328241	H 2.352634 0.925717 0.475932
4et	V -0.296146 0.089535 -0.012972	V -0.260306 0.091982 0.000007	V 0.031542 0.173765 0.000469
e-type	O -0.679051 1.627306 0.016353	O 0.685750 1.461942 -0.000010	O 1.775489 0.162151 0.000007
	O -1.136000 -1.590172 0.013767	O -2.007417 -0.518712 -0.000009	O -1.364294 1.345238 -0.000575
	C 2.123344 -0.235501 0.012759	C 1.616913 -1.007756 -0.000007	C -0.672632 -1.718947 -0.000292
	H 2.996221 -0.283032 -0.630900	H 2.236678 -1.091009 -0.890255	H -0.491236 -2.308372 -0.896867
	H 2.418477 -0.306852 1.054489	H 2.236637 -1.090994 0.890270	H -0.490879 -2.309445 0.895493
	H 1.507540 -1.106107 -0.261052	H 0.950463 -1.885416 -0.000009	H -1.724273 -1.373515 0.000091
	H 1.669473 0.752632 -0.181705	H 1.435123 0.452540 0.000016	H 2.727142 0.249316 -0.003204
2et	V 1.124319 -0.043271 0.006003	V 0.851995 -0.281398 0.000031	V 1.021474 -0.000010 0.000831
i-type	O 0.175425 -1.326016 -0.011210	O 1.476303 1.179162 -0.000049	O 2.621736 0.000215 -0.001883
	O 0.411935 1.385804 -0.010344	O -0.775899 -1.133066 -0.000058	O -0.803764 -0.000413 0.001668
	C -3.056485 0.051803 0.003419	C -2.543030 0.641833 0.000020	C -4.020717 0.000211 -0.001886
	H -3.645362 0.199317 0.906348	H -3.124732 0.519213 -0.906781	H -4.035804 0.935355 -0.533622
	H -2.219241 0.746098 -0.005607	H -1.756913 -0.326858 -0.000093	H -1.764328 -0.000125 0.002088
	H -3.685531 0.224340 -0.867383	H -3.124263 0.519466 0.907155	H -4.036163 -0.927237 -0.546921
	H -2.669177 -0.963652 -0.019501	H -1.935027 1.540562 -0.000259	H -4.077092 -0.007448 1.072374
2et	V -0.248031 -0.000020 0.185018	V -0.821503 -0.225415 0.250320	V 1.021397 -0.001315 -0.000135
p-type	O -0.955062 1.385866 -0.203694	O -1.873882 0.814386 -0.319083	O 2.621669 0.003920 -0.001847
	O -0.956334 -1.385245 -0.203740	O 0.711419 -0.686732 -0.525560	O -0.803805 -0.002096 0.002740
	C 2.086336 -0.000425 -0.092080	C 2.861036 0.442672 0.118874	C -4.020625 0.001821 -0.000932
	H 3.082563 -0.000426 -0.520767	H 3.569936 0.107806 -0.629483	H -4.064471 -0.814138 -0.700687
	H 1.605439 -0.919306 -0.462719	H 1.757001 -0.191717 -0.261850	H -1.764354 -0.000749 0.002167
	H 1.607532 0.921756 -0.457035	H 2.618814 1.496648 0.056977	H -4.025614 -0.196963 1.056426
	H 2.182327 -0.003987 0.997069	H 3.082295 0.094531 1.120887	H -4.056861 1.016578 -0.356361

Table A6 – CrO_2 reaction paths in order of increasing E_a

System	Reactant Interacting Complex	Transition State	Product Interacting Complex
5et	Cr -0.824136 0.080795 -0.000049	Cr 0.821863 -0.260657 -0.000002	Cr -1.002623 -0.209161 -0.000276
i-type	O -0.691543 -1.483730 0.000111	O 1.353090 1.220463 0.000003	O -2.268946 0.740292 0.000312
	O 0.109967 1.654846 0.000073	O -0.711715 -1.182171 0.000003	O 0.730445 -0.471567 0.001024
	C 2.441844 -0.332972 -0.000017	C -2.502507 0.620118 -0.000001	C 3.845440 0.339893 -0.000766
	H 3.528946 -0.296454 0.002882	H -3.092670 0.525132 -0.905355	H 3.998988 -0.135015 0.952519
	H 2.076566 0.182109 -0.888595	H -1.779655 -0.327329 0.000008	H 1.659559 -0.211781 0.003632

	H 2.072396 0.169561 0.893950	H -3.092843 0.525003 0.905226	H 3.998916 -0.217726 -0.908183
	H 2.102884 -1.365391 -0.008428	H -1.875498 1.505925 0.000120	H 3.640864 1.395237 -0.047430
5et e-type	Cr 0.432246 -0.050573 -0.000011	Cr 0.663750 -0.118642 0.000001	Cr 1.002841 -0.208933 -0.000045
	O -0.282325 1.645238 0.000008	O -0.742118 1.027629 -0.000000	O -0.731239 -0.464711 0.000120
	O 1.865673 -0.697453 0.000017	O 2.236654 -0.175606 -0.000002	O 2.272154 0.736414 0.000054
	C -2.296917 -0.639285 0.000012	C -2.814031 -0.420540 -0.000000	C -3.848213 0.335703 -0.000169
	H -3.384644 -0.648015 -0.000018	H -3.356681 -0.179033 -0.907129	H -3.684493 1.339851 -0.350268
	H -1.929823 -1.664249 0.000787	H -2.424405 -1.434129 -0.000093	H -4.038572 -0.454180 -0.705715
	H -1.972370 -0.109593 0.899365	H -3.356576 -0.179156 0.907224	H -3.924055 0.141432 1.055459
	H -1.972353 -0.110964 -0.900136	H -1.864439 0.346791 -0.000006	H -1.659112 -0.200545 0.001238
5et e-type	Cr -0.228392 0.075302 -0.006067	Cr 0.245477 0.053170 0.000030	Cr 0.093278 0.073865 -0.020856
	O -0.562008 1.637285 0.007075	O -0.615261 1.483861 -0.000030	O 1.394889 -1.110331 -0.079273
	O -1.413770 -1.391857 0.006817	O 2.019971 -0.515366 -0.000036	O 0.191746 1.909776 0.031783
	C 2.119151 -0.376842 0.007698	C -1.661712 -0.952291 -0.000012	C -1.751401 -0.700999 0.022923
	H 2.567325 -0.495168 0.988192	H -1.516775 -1.559506 -0.894640	H -1.997139 -1.092699 1.010682
	H 1.420396 -1.213257 -0.160775	H -1.516889 -1.559706 0.894499	H -2.445643 0.104808 -0.227550
	H 2.869994 -0.452749 -0.772074	H -2.705630 -0.638754 -0.000047	H -1.840599 -1.495870 -0.718842
	H 1.715012 0.651558 -0.067067	H -1.419555 0.447676 0.000073	H 1.860040 -1.478574 0.678643
3et e-type	Cr 0.277339 -0.000045 0.000083	Cr -0.303433 0.037294 -0.000384	Cr -0.089868 -0.139989 0.000401
	O 0.911615 -1.456580 -0.000093	O 0.497439 1.493173 0.000351	O -1.561138 0.813764 -0.000319
	O 0.917060 1.454070 -0.000107	O -1.743175 -0.591558 0.000551	O 0.250535 -1.650415 -0.000478
	C -2.119076 0.002059 -0.000125	C 1.674860 -0.863633 0.000204	C 1.586844 0.964101 -0.000188
	H -2.734541 0.002585 0.893094	H 1.569120 -1.478534 0.893823	H 2.186282 0.749525 0.883757
	H -1.552109 0.950844 0.002156	H 1.568074 -1.478762 -0.893171	H 2.175221 0.763250 -0.894777
	H -2.730260 0.003237 -0.896249	H 2.697577 -0.483688 -0.000517	H 1.276348 2.010596 0.009557
	H -1.554190 -0.947864 0.001364	H 1.364343 0.514793 0.000644	H -2.517259 0.744958 -0.000649
1et p-type	Cr -0.252613 -0.000037 -0.000002	Cr 0.295703 0.067875 -0.189196	Cr -0.085381 -0.131261 -0.000735
	O -0.948318 1.416911 0.000016	O -0.445727 1.495475 0.188513	O -1.577244 0.778468 0.000335
	O -0.952773 -1.414763 -0.000015	O 1.600509 -0.666717 0.265484	O 0.278835 -1.633734 0.000866
	C 2.117941 -0.001596 -0.000013	C -1.590812 -0.874408 0.064651	C 1.567562 0.966272 0.000514
	H 2.730425 -0.003887 -0.895356	H -2.387330 -0.688109 0.785268	H 1.238164 2.007511 0.000583
	H 2.730409 -0.000691 0.895354	H -2.032517 -1.061936 -0.912403	H 2.160590 0.762736 0.891821
	H 1.550549 -0.950352 0.001753	H -1.072729 -1.769570 0.416861	H 2.161426 0.763036 -0.890324
	H 1.552417 0.948201 -0.001633	H -1.297685 0.507010 0.231095	H -2.529128 0.661473 0.002869
3et i-type	Cr 1.109580 -0.270211 0.000401	Cr -0.880142 -0.265183 0.000005	Cr 1.001336 -0.209157 -0.000092
	O 2.360611 0.703355 0.000051	O -2.001585 0.864749 -0.000006	O 2.267210 0.741590 0.000095
	O -0.466580 -0.084275 -0.001805	O 0.786394 -0.537015 -0.000011	O -0.730954 -0.473621 0.000196
	C -4.177309 0.153113 0.000432	C 3.131573 0.393891 0.000001	C -3.839573 0.340892 -0.000084
	H -4.542550 -0.058710 1.002801	H 3.574720 0.001508 -0.907787	H -3.915470 0.155819 1.057201
	H -3.089997 0.146081 -0.001534	H 1.927431 -0.098696 -0.000010	H -1.660542 -0.214091 0.000477

	H -4.535981 1.130546 -0.313618 H -4.549776 -0.604162 -0.685840	H 2.981801 1.467088 -0.004822 H 3.571545 0.009273 0.912643	H -3.664379 1.340234 -0.358296 H -4.044281 -0.451302 -0.699008
1et i-type	Cr 0.273552 0.000127 0.161629 O 0.875543 -1.418650 -0.191488 O 0.867830 1.422143 -0.191326 C -2.041117 -0.003100 -0.067172 H -2.538941 -0.006675 0.897443 H -1.480753 0.937740 -0.217674 H -2.771234 -0.003758 -0.871332 H -1.474607 -0.939700 -0.221987	Cr 0.843292 -0.261173 -0.037881 O 1.275804 1.242438 0.061888 O -0.677708 -1.132830 0.079700 C -2.527622 0.569827 -0.025029 H -3.053161 0.404730 -0.958787 H -1.708506 -0.352254 0.038882 H -3.146167 0.432257 0.854933 H -1.950211 1.487591 -0.008413	Not found

Table A7 – H_3N-TiO_2 reaction paths in order of increasing E_a

System	Reactant Interacting Complex	Transition State	Product Interacting Complex
3et i-type	Ti 0.537218 -0.136411 0.000006 O 0.076407 1.417082 0.000120 O -0.760771 -1.517813 -0.000090 C -3.492666 0.300562 -0.000041 H -4.093219 0.485686 -0.888151 H -3.154557 -0.734119 -0.000087 H -4.093309 0.485577 0.888030 H -2.628474 0.961511 0.000043 N 2.754328 0.044863 0.000003 H 2.956964 0.619809 -0.817310 H 2.956973 0.619713 0.817382 H 3.387426 -0.748700 -0.000047	Ti -0.437832 -0.072729 0.000089 O -0.233664 1.541647 0.000036 O 1.034278 -1.223760 0.000053 C 3.113730 0.186090 -0.000118 H 3.671377 -0.030058 0.905026 H 2.179145 -0.600068 -0.000031 H 3.671385 -0.030273 -0.905207 H 2.660819 1.171729 -0.000235 N -2.655924 -0.274317 -0.000138 H -2.952416 0.257412 0.817588 H -2.952204 0.257410 -0.817941 H -3.141636 -1.165526 -0.000200	Ti 0.479967 -0.115949 -0.000230 O 0.031708 1.452431 -0.000597 O -0.736337 -1.504386 -0.000387 C -3.471196 0.419058 0.000691 H -3.953912 0.170105 -0.928589 H -1.692175 -1.595251 -0.000598 H -3.951458 0.168165 0.930723 H -2.539467 0.960867 0.000020 N 2.700877 0.040393 0.000684 H 2.906721 0.613531 -0.816742 H 2.906153 0.613461 0.818302 H 3.322931 -0.761467 0.000868
1et p-type	Ti -0.009412 0.142944 -0.000062 O -0.210677 1.012382 1.387071 O -0.210409 1.008942 -1.389369 C 2.291993 -0.794392 0.000900 H 3.347737 -1.041688 0.000807 H 1.730429 -1.734248 0.001102 H 2.096228 -0.215427 -0.909922 H 2.096213 -0.215075 0.911431 N -1.839910 -1.105076 0.001089 H -2.048580 -1.651392 0.830718 H -2.470478 -0.302720 0.000173 H -2.048380 -1.652926 -0.827583	Ti -0.041130 -0.178772 0.018563 O 0.622069 0.221925 -1.518587 O -0.443938 -1.735131 0.287980 C 1.969017 0.601754 0.733725 H 2.869706 1.061674 0.329034 H 1.550473 1.325913 1.444954 H 2.282424 -0.286947 1.283622 H 1.494889 0.515778 -0.593603 N -1.953009 0.938572 0.259114 H -2.107650 1.457720 -0.602066 H -2.659783 0.208775 0.320354 H -2.093285 1.575198 1.038040	Ti -0.070467 0.184679 -0.106047 O -1.361953 1.052757 0.860579 O -0.258806 0.106149 -1.705278 C 1.942523 0.592773 0.415572 H 2.180483 1.620060 0.119709 H 2.117509 0.516677 1.493952 H 2.657349 -0.053963 -0.101567 H -2.170172 1.534884 0.679687 N -0.189796 -1.944470 0.425073 H -0.235791 -2.148401 1.419092 H -0.999499 -2.357122 -0.030988 H 0.639899 -2.391673 0.041786

Table A8 – H_3N-VO_2 reaction paths in order of increasing E_a

System	Reactant Interacting Complex			Transition State			Product Interacting Complex		
4et i-type	V	0.681387	-0.053760	0.075320	V	0.408425	0.092566	0.000084	V	-0.658133	-0.256950	-0.000285
	O	0.827780	0.366478	1.606707	O	0.544329	1.685968	0.000040	O	-1.657462	-1.515037	0.000482
	O	0.928655	-1.581292	-1.006180	O	-0.964507	-1.148230	0.000216	O	1.080448	0.261245	-0.001080
	C	-2.619745	-0.596474	0.284644	C	-3.178917	0.033931	-0.000193	C	4.304961	0.101687	0.000827
	H	-3.364020	-1.260167	0.717162	H	-3.708820	-0.242939	0.904901	H	4.339291	0.587793	0.959862
	H	-1.997208	-1.167195	-0.405097	H	-2.167283	-0.645591	0.000015	H	2.038976	0.209878	-0.000498
	H	-2.005038	-0.182189	1.084149	H	-2.857159	1.070165	-0.000294	H	4.262649	-0.971656	-0.056215
	H	-3.132389	0.204989	-0.246784	H	-3.708587	-0.243145	-0.905359	H	4.361456	0.686256	-0.900396
	N	-0.297192	1.604787	-0.907896	N	2.441228	-0.639226	-0.000203	N	-2.027005	1.411532	0.000317
	H	-0.411672	2.258621	-0.135521	H	2.959589	0.237250	0.000995	H	-2.921447	0.926353	-0.000893
	H	-1.223693	1.367142	-1.253668	H	2.717562	-1.166779	-0.823135	H	-1.983668	2.006473	-0.821279
	H	0.209456	2.079141	-1.649409	H	2.717234	-1.168879	0.821487	H	-1.984821	2.004248	0.823582
4et e-type	V	-0.608338	-0.223119	0.000253	V	0.593343	-0.275529	-0.000072	V	0.658173	-0.257070	0.000033
	O	-2.176597	0.034623	-0.000293	O	2.180922	-0.426966	-0.001453	O	1.657907	-1.514839	-0.000147
	O	0.363932	-1.837143	-0.000239	O	-0.868848	-1.457924	0.002087	O	-1.080495	0.260857	0.000259
	C	2.725957	0.027164	0.000047	C	-2.723854	0.198179	-0.001462	C	-4.305011	0.101908	-0.000035
	H	2.140884	-0.190542	0.894595	H	-2.570101	0.765413	-0.914006	H	-4.269197	-0.972064	-0.048988
	H	2.139918	-0.194475	-0.893059	H	-1.878344	-0.746312	0.000387	H	-2.039019	0.209323	0.000128
	H	3.600211	-0.617322	0.000950	H	-3.671725	-0.328831	0.005274	H	-4.341160	0.595502	0.955095
	H	3.042124	1.069124	-0.003029	H	-2.563204	0.775896	0.903310	H	-4.353047	0.679991	-0.905957
	N	0.104286	1.825631	-0.000026	N	0.284596	1.867666	0.001092	N	2.026633	1.411748	-0.000156
	H	-0.780725	2.328828	-0.000896	H	1.248056	2.197541	-0.011926	H	2.921216	0.926827	-0.000118
	H	0.632797	2.106120	-0.821183	H	-0.167260	2.245145	0.829026	H	1.983813	2.005747	0.822153
	H	0.632151	2.107747	0.820969	H	-0.189952	2.244685	-0.814348	H	1.983741	2.005451	-0.822678
2et p-type	V	0.213067	-0.287906	0.000013	V	0.044894	-0.332231	0.069871	V	-0.240901	0.014720	-0.176827
	O	0.790091	-0.756086	1.438717	O	-1.095670	-0.395801	1.321365	O	-1.706092	-0.158887	0.856443
	O	0.791779	-0.757015	-1.437660	O	0.588112	-1.492670	-0.888936	O	-0.063151	-0.145723	-1.738460
	C	-2.254547	-0.059889	-0.000619	C	-1.368421	1.116426	-0.824045	C	0.891890	1.627514	0.434511
	H	-3.050059	-0.798117	-0.000140	H	-2.443662	1.031297	-0.975916	H	0.488118	2.568868	0.058135
	H	-2.669837	0.943505	-0.001698	H	-1.124124	2.159528	-0.622442	H	0.860264	1.659540	1.529855
	H	-1.693468	-0.218222	-0.935484	H	-0.912281	0.826873	-1.777146	H	1.936038	1.556501	0.118492
	H	-1.694045	-0.216481	0.934862	H	-1.488041	0.440727	0.415877	H	-2.642247	-0.348604	0.783289
	N	0.474929	1.835788	-0.000213	N	1.635641	1.092005	0.278258	N	1.284912	-1.255000	0.571744
	H	1.035773	2.030035	0.825779	H	1.976771	1.169357	1.232582	H	1.040926	-2.236050	0.670381
	H	-0.320656	2.466547	-0.002812	H	1.381140	2.023612	-0.039308	H	1.629447	-0.907197	1.462432
	H	1.039583	2.028194	-0.824070	H	2.399133	0.755088	-0.303644	H	2.036396	-1.174819	-0.108700

Table A9 – H_3N-CrO_2 reaction paths in order of increasing E_a

System	Reactant Interacting Complex			Transition State			Product Interacting Complex		
5et p-type	Cr	-0.435930	0.333362 -0.022646	Cr	-0.377743	0.141113 -0.218140	Cr	-0.682017	-0.089125 0.006965
	O	0.547348	1.367805 -1.273707	O	1.038943	-0.732548 -1.054548	O	-2.490540	0.057055 -0.097041
	O	-0.859802	0.644537 1.495927	O	-0.548449	1.711528 0.079942	O	0.228634	-1.422105 -0.003603
	C	2.342454	-0.679791 0.424821	C	2.669829	-0.172355 0.752387	C	3.372228	-0.321443 -0.001789
	H	1.703992	-0.607124 1.306470	H	2.167800	0.677363 1.206091	H	2.512508	-0.976189 0.002067
	H	1.994088	-1.471860 -0.239216	H	2.752815	-1.025848 1.416964	H	3.855366	-0.053169 0.922893
	H	3.357329	-0.910668 0.740459	H	3.613946	0.104298 0.295174	H	3.841176	-0.046673 -0.931851
	H	2.342571	0.269706 -0.112059	H	1.976820	-0.547776 -0.206942	H	-3.127781	-0.177256 0.581370
	N	-1.020002	-1.627105 -0.528259	N	-2.050168	-0.892066 0.538017	N	0.634920	1.549126 0.008212
	H	-2.018703	-1.757068 -0.389000	H	-2.888140	-0.639922 0.020212	H	0.569940	2.137437 -0.818022
	H	-0.537961	-2.271753 0.094230	H	-2.192809	-0.604017 1.502987	H	1.563266	1.108599 0.010682
	H	-0.794075	-1.882171 -1.486266	H	-1.956340	-1.904061 0.517276	H	0.571366	2.151420 0.824094
1et p-type	Cr	0.206547	-0.290603 -0.000259	Cr	0.050313	-0.337614 0.085466	Cr	-0.076810	0.246508 -0.124490
	O	0.717249	-0.716554 1.446310	O	-1.046041	-0.353567 1.339377	O	-1.577383	0.371501 0.856533
	O	0.720961	-0.711763 -1.446941	O	0.730256	-1.401463 -0.853871	O	0.240755	0.747596 -1.569997
	C	-2.156085	-0.011756 -0.001565	C	-1.326382	0.954098 -0.919943	C	1.587491	0.349406 0.983944
	H	-1.591874	-0.155125 -0.938569	H	-0.781343	0.643922 -1.817015	H	2.414534	-0.198468 0.526820
	H	-2.935849	-0.766826 -0.003203	H	-2.377360	0.744945 -1.117612	H	1.903556	1.376505 1.168175
	H	-2.588900	0.985086 -0.000749	H	-1.189477	2.027013 -0.782375	H	1.341387	-0.118180 1.943690
	H	-1.593501	-0.157445 0.936075	H	-1.461673	0.391430 0.387206	H	-2.204932	1.097740 0.882319
	N	0.485676	1.755185 0.002668	N	1.430669	1.187260 0.282094	N	-0.041080	-1.808278 -0.169517
	H	1.045670	1.949190 -0.823556	H	2.298549	0.846678 -0.124120	H	-0.050221	-2.127443 -1.134119
	H	1.051030	1.946863 0.825761	H	1.604170	1.406902 1.259037	H	-0.881309	-2.143034 0.296402
	H	-0.312614	2.383501 0.006224	H	1.169513	2.046669 -0.195367	H	0.776069	-2.194580 0.295141
1et p-type	Cr	0.207785	-0.290040 -0.000350	Cr	-0.545377	-0.249109 0.108109	Cr	-0.075757	-0.246766 0.124177
	O	0.721681	-0.715258 1.445291	O	-1.424496	-1.409798 -0.489249	O	0.244506	-0.752088 1.567612
	O	0.721241	-0.709149 -1.447979	O	1.053607	-0.314782 0.783395	O	-1.575602	-0.375729 -0.857199
	C	-2.155460	-0.017933 0.000146	C	3.196708	0.299575 -0.421979	C	1.588439	-0.340603 -0.985096
	H	-1.592025	-0.163616 0.937215	H	2.972379	0.000813 -1.438084	H	2.414831	0.204707 -0.523789
	H	-1.591556	-0.160222 -0.937214	H	2.037852	-0.061311 0.294190	H	-2.199324	-1.105300 -0.885057
	H	-2.589607	0.978334 0.001608	H	3.290861	1.367067 -0.266643	H	1.904883	-1.366552 -1.175316
	H	-2.934133	-0.774131 -0.001397	H	3.950928	-0.299690 0.072204	H	1.343489	0.132949 -1.942162
	N	0.478769	1.756817 0.002859	N	-1.479157	1.606211 -0.096170	N	-0.048959	1.808225 0.173797
	H	1.043724	1.951101 0.825606	H	-2.470868	1.394489 -0.181607	H	0.765794	2.199678 -0.290747
	H	-0.322531	2.381279 0.006968	H	-1.195311	2.116215 -0.929406	H	-0.059452	2.126270 1.138762
	H	1.037284	1.953342 -0.823765	H	-1.355825	2.216752 0.706621	H	-0.891218	2.139212 -0.291242

Table A10 – Cl-TiO_2 reaction paths in order of increasing E_a

System	Reactant Interacting Complex			Transition State			Product Interacting Complex		
4et e-type	Ti	0.094184	-0.528882	0.092345	Ti	-0.622168	-0.344941	0.000320	Ti	0.459972	-0.373882	0.000136
	O	0.623483	-1.912317	-1.005683	O	-2.394005	-0.886169	-0.002065	O	1.052099	-2.130343	-0.000444
	O	-1.338712	-0.882026	1.233544	O	0.689147	-1.591532	0.002348	O	-1.292791	-0.201100	0.000710
	C	-2.137606	1.349213	-0.658036	C	2.932602	-0.315504	-0.001681	C	-4.340898	0.575093	-0.000334
	H	-1.692046	1.480287	0.331981	H	2.879536	0.287946	-0.901429	H	-4.293914	1.152855	0.906305
	H	-2.562343	0.351374	-0.763559	H	1.981276	-1.005268	0.000299	H	-2.215909	0.087926	0.000289
	H	-1.395258	1.536115	-1.432509	H	2.884792	0.284974	0.900347	H	-4.309592	1.071642	-0.954520
	H	-2.939501	2.078160	-0.751246	H	3.767119	-1.009944	-0.005313	H	-4.541303	-0.481399	0.047403
	Cl	1.474386	1.202878	0.159358	Cl	-0.104810	1.808566	0.000404	Cl	1.953662	1.270316	-0.000153
4et i-type	Ti	0.020964	0.000007	-0.089844	Ti	-0.160375	0.061964	0.000734	Ti	0.459946	0.373823	0.000004
	O	-0.660088	1.698343	-0.409976	O	0.603474	1.759029	0.001353	O	1.051915	2.130318	0.000006
	O	-0.660273	-1.698288	-0.409993	O	0.939505	-1.375957	0.002477	O	-1.292836	0.201163	-0.000015
	C	-2.727816	0.000020	0.467942	C	3.157995	-0.130826	-0.002491	C	-4.341054	-0.575258	-0.000000
	H	-1.925068	0.000187	1.215255	H	2.851270	0.912002	0.000622	H	-4.542910	0.482009	-0.007328
	H	-2.375358	-0.000148	-0.569293	H	2.162568	-0.827942	-0.000434	H	-2.216029	-0.087606	-0.000021
	H	-3.315571	0.900360	0.618590	H	3.676125	-0.421166	0.904836	H	-4.299821	-1.119086	-0.927666
	H	-3.315488	-0.900331	0.618860	H	3.670270	-0.417353	-0.914310	H	-4.302367	-1.106664	0.934946
	Cl	2.200003	-0.000046	0.226191	Cl	-2.360222	-0.169905	-0.001328	Cl	1.953882	-1.270180	0.000003
2et i-type	Ti	0.306949	0.034566	-0.003083	Ti	-0.197432	0.095911	0.000654	Ti	0.237806	0.046503	0.000028
	O	-0.430180	1.439795	-0.016518	O	0.404167	1.570097	-0.000016	O	-0.439283	1.486204	0.000035
	O	-0.915193	-1.321227	-0.020007	O	1.077827	-1.183341	0.000483	O	-0.951253	-1.301380	0.000053
	C	-3.917424	0.009428	0.016968	C	3.389739	-0.104303	-0.000801	C	-3.803045	0.081811	-0.000071
	H	-4.579109	0.172976	-0.830253	H	3.901412	-0.413069	0.904420	H	-4.217084	-0.267787	-0.930042
	H	-3.510232	-0.998507	-0.031215	H	2.358474	-0.709235	-0.000161	H	-1.919439	-1.267144	0.000077
	H	-4.476763	0.129250	0.941712	H	3.901910	-0.415922	-0.904762	H	-4.217333	-0.267665	0.929834
	H	-3.106769	0.734542	-0.012145	H	3.110329	0.943709	-0.002498	H	-3.063625	0.865910	-0.000022
	Cl	2.540442	-0.106108	0.011184	Cl	-2.419001	-0.234339	-0.000607	Cl	2.478135	-0.120931	-0.000043
2et i-type	Ti	-0.264320	0.007981	-0.000001	Ti	0.197451	0.095915	-0.000086	Ti	0.237764	0.046647	-0.000020
	O	0.559037	-1.347892	-0.000047	O	-0.404130	1.570101	-0.000006	O	-0.438956	1.486520	-0.000105
	O	0.868652	1.440241	-0.000042	O	-1.077874	-1.183282	-0.000076	O	-0.951679	-1.300793	0.000134
	C	3.694920	-0.101653	0.000039	C	-3.389820	-0.104326	0.000116	C	-3.802662	0.081429	0.000161
	H	3.262144	0.355689	0.887800	H	-3.110549	0.943726	-0.000187	H	-3.062674	0.864969	0.000049
	H	3.262106	0.355530	-0.887786	H	-2.358450	-0.709077	-0.000050	H	-1.919915	-1.267320	0.000172
	H	3.476943	-1.166347	0.000132	H	-3.901956	-0.414793	-0.904261	H	-4.217162	-0.267813	-0.929711
	H	4.770267	0.059395	0.000002	H	-3.901439	-0.414396	0.904920	H	-4.217031	-0.267670	0.930145
	Cl	-2.502791	0.005369	0.000021	Cl	2.419024	-0.234364	0.000084	Cl	2.478060	-0.121340	-0.000083

2et e-type	Ti -0.239085 -0.281913 0.051336 O -0.791004 -0.894512 1.416250 O -1.082133 -1.199398 -1.278209 C -1.276272 1.916695 -0.079751 H -0.593411 1.918461 0.778696 H -2.036492 1.128345 -0.001704 H -0.732314 1.876200 -1.027401 H -1.813211 2.858550 -0.050572 Cl 1.945766 0.215980 -0.085543	Ti 0.475375 -0.476930 0.000141 O 1.710582 -1.473594 -0.000196 O -1.095522 -1.393094 -0.000048 C -2.890288 0.391769 -0.000044 H -3.462862 0.234857 0.907110 H -2.076908 -0.537292 -0.000004 H -2.324329 1.317595 0.000645 H -3.461868 0.235689 -0.907963 Cl 0.781704 1.754382 -0.000039	Ti -0.666565 -0.358247 0.000046 O -2.179652 -0.836016 0.000840 O 0.501565 -1.741352 -0.001019 C 3.310268 -0.125161 0.000767 H 2.740841 0.788935 0.001610 H 1.467649 -1.704926 -0.001829 H 3.644463 -0.550262 0.931538 H 3.646201 -0.547401 -0.930678 Cl -0.192449 1.839117 -0.000284
2et p-type	Ti 0.238829 0.281935 0.051199 O 0.794618 0.888312 1.417424 O 1.079958 1.203296 -1.276256 C 1.276522 -1.915600 -0.080841 H 1.810780 -2.857605 -0.138655 H 0.617224 -1.963098 0.792710 H 0.707130 -1.821758 -1.011444 H 2.039614 -1.133666 0.023243 Cl -1.946160 -0.215631 -0.084501	Ti 0.187384 0.218492 0.051637 O 1.068768 0.003036 1.463485 O 0.744390 1.773992 -0.714493 C 1.446148 -1.405579 -0.717907 H 2.293362 -1.971683 -0.329819 H 0.651645 -2.120560 -0.943046 H 1.778081 -0.917440 -1.635348 H 1.519183 -0.793440 0.632771 Cl -1.973346 -0.281556 -0.032063	Ti 0.279495 0.098644 -0.046062 O 1.176370 1.143864 1.037102 O 0.858229 0.459219 -1.741196 C 0.933824 -1.797124 0.344462 H 2.019362 -1.840779 0.251057 H 0.633156 -2.078316 1.355569 H 0.471896 -2.473290 -0.378289 H 1.450159 1.759669 1.718466 Cl -1.917835 0.024743 0.096032

Table A11 – Cl-VO_2 reaction paths in order of increasing E_a

System	Reactant Interacting Complex	Transition State	Product Interacting Complex
3et i-type	V 0.255867 0.053043 0.000026 O -0.417074 1.454540 0.000281 O -0.879405 -1.327876 -0.000097 C -3.643990 -0.010357 0.000029 H -4.687240 0.296889 0.000044 H -3.585047 -1.096249 -0.000049 H -3.152744 0.383292 0.887378 H -3.152734 0.383418 -0.887259 Cl 2.407564 -0.125795 -0.000138	V 0.187392 0.093042 0.000011 O -0.391844 1.542362 0.000138 O -1.002011 -1.210622 -0.000073 C -3.307054 -0.088140 0.000051 H -4.101079 -0.827699 -0.000081 H -2.305845 -0.722643 -0.000016 H -3.276254 0.512489 0.902280 H -3.276204 0.512762 -0.901994 Cl 2.331914 -0.219997 -0.000074	V 0.238546 0.071124 -0.001539 O -0.350655 1.515627 -0.000874 O -0.919235 -1.246382 -0.002161 C -3.781603 0.030560 0.002931 H -4.179233 -0.337599 -0.926987 H -1.889475 -1.203699 -0.001750 H -4.171720 -0.342504 0.934077 H -3.094265 0.860606 0.002204 Cl 2.393933 -0.173528 0.002033
3et e-type	V -0.377661 -0.284008 0.077487 O -1.013042 -0.614656 1.462021 O -1.179169 -0.906395 -1.422526 C -0.472390 2.174963 -0.129606 H -0.443327 1.571201 -1.046584 H 0.444027 2.753050 -0.091026 H -0.548490 1.634014 0.829809 H -1.355288 2.802972 -0.192427	V -0.546702 0.394632 0.001130 O -1.955668 1.054295 -0.003084 O 0.802535 1.545384 0.001548 C 2.820393 -0.003014 -0.001617 H 2.690819 -0.581898 -0.909099 H 1.930773 0.824007 0.001040 H 3.717949 0.606743 0.002989 H 2.687857 -0.591460 0.899278	V -0.683204 -0.317255 -0.000168 O -2.205556 -0.638166 0.000461 O 0.406949 -1.698516 -0.000172 C 3.227424 -0.243082 0.000210 H 2.887177 0.181229 0.929482 H 1.375657 -1.713535 -0.000018 H 3.995439 -0.997082 0.000228 H 2.887348 0.181391 -0.929049

	Cl 1.821253 -0.182966 -0.048253	Cl -0.361797 -1.771370 0.000106	Cl -0.023978 1.752754 -0.000021
3et p-type	V 0.377614 0.284082 -0.077395	V -0.112422 -0.397337 0.111785	V 0.395423 -0.200343 0.177904
	O 1.180446 0.905027 1.422526	O -1.312609 0.247657 1.352407	O 1.420027 -0.890421 -1.110040
	O 1.012029 0.615859 -1.462089	O -0.444494 -1.722630 -0.637524	O 0.903885 0.133210 1.617477
	C 0.472370 -2.175103 0.128387	C -1.554746 1.288880 -0.843046	C 0.076466 2.044891 -0.600373
	H -0.443188 -2.754486 0.088446	H -1.191895 2.306741 -0.780565	H 0.083189 1.691335 -1.621712
	H 0.548827 -1.633840 -0.830873	H -0.896979 0.681065 -1.490324	H -0.853559 2.386552 -0.178927
	H 1.355978 -2.801926 0.191935	H -2.577600 1.174539 -1.180706	H 1.006252 2.310670 -0.117770
	H 0.441096 -1.571588 1.045387	H -1.679357 0.930574 0.382398	H 2.330667 -1.167765 -1.227895
	Cl -1.821286 0.183028 0.048904	Cl 1.900991 0.477196 -0.009568	Cl -1.806551 -0.401445 -0.082515
1et p-type	V -0.189016 -0.300678 -0.000982	V 0.190181 0.251820 0.015172	V -0.276501 -0.103352 -0.124007
	O -0.591995 -1.201945 1.221345	O 1.029565 0.261983 1.437440	O -1.101071 -1.382659 0.738978
	O -0.684274 -0.953526 -1.339896	O 0.540035 1.474568 -0.885115	O -0.747847 -0.066161 -1.596678
	C -1.686617 1.605605 0.086552	C 1.475873 -1.370342 -0.574339	C -1.020491 1.589269 0.630395
	H -2.095162 2.264544 0.846083	H 2.185955 -1.970518 -0.002235	H -0.755936 1.634826 1.686426
	H -0.598701 1.789751 0.106637	H 0.664164 -2.034503 -0.874744	H -0.556835 2.405828 0.076740
	H -2.064825 1.843293 -0.900283	H 1.990216 -0.962575 -1.438717	H -2.099430 1.599279 0.490862
	H -2.034154 0.597401 0.370747	H 1.501617 -0.647166 0.687625	H -0.887604 -1.703211 1.622570
	Cl 1.851180 0.472396 0.001676	Cl -1.889891 -0.343968 0.018032	Cl 1.857272 0.029136 0.120870
1et l-type	V 0.473571 0.400527 0.199803	V 0.366296 0.416289 0.000068	V -0.384680 0.309092 -0.000155
	O 0.685956 1.862868 -0.315384	O 0.800431 1.914584 -0.000181	O -0.497760 1.864193 0.000184
	O -1.036181 -0.000265 0.138067	O -1.290219 0.190912 0.000240	O 1.193311 -0.428748 -0.000398
	C -4.231038 -0.543595 -0.114061	C -3.656656 -0.662320 -0.000131	C 4.314360 -0.438219 0.000274
	H -3.674296 -1.335328 -0.608978	H -4.215827 0.265356 0.004247	H 4.453836 0.097758 -0.922365
	H -3.928141 0.415019 -0.527193	H -2.426867 -0.246278 0.000004	H 2.156959 -0.323785 -0.000105
	H -4.004969 -0.560697 0.949405	H -3.738466 -1.237522 -0.914282	H 4.446240 0.069718 0.939756
	H -5.297473 -0.692323 -0.264878	H -3.736269 -1.244813 0.909582	H 4.172043 -1.505164 -0.016324
	Cl 2.011809 -1.098708 -0.120054	Cl 1.855933 -1.175378 -0.000047	Cl -2.225412 -0.841287 0.000157
1et i-type	V 0.239337 -0.288190 -0.000109	V 0.169703 0.086244 0.000041	V 0.384734 0.309034 0.000018
	O 0.715693 -1.052725 1.286221	O -0.422547 1.529988 -0.000099	O 0.499382 1.863989 -0.000032
	O 0.717909 -1.054721 -1.284534	O -0.982353 -1.240536 -0.000118	O -1.193766 -0.427837 0.000132
	C 1.424843 1.729116 -0.000195	C -3.242554 -0.070372 0.000068	C -4.315052 -0.437983 -0.000082
	H 2.125745 2.557295 -0.003203	H -4.018695 -0.828210 -0.000144	H -4.173872 -1.505213 0.000058
	H 2.064313 0.829757 0.002550	H -2.212793 -0.722125 -0.000112	H -2.157541 -0.323521 0.000184
	H 0.821191 1.812623 -0.908853	H -3.206671 0.525607 0.904432	H -4.450327 0.084166 0.931079
	H 0.822225 1.817944 0.908520	H -3.206644 0.526042 -0.904004	H -4.450121 0.083948 -0.931395
	Cl -1.844477 0.358566 -0.000519	Cl 2.319774 -0.198724 0.000012	Cl 2.225197 -0.841675 -0.000039

Table A12 – Cl-CrO_2 reaction paths in order of increasing E_a

System	Reactant Interacting Complex	Transition State	Product Interacting Complex
4et e-type	Cr 0.799718 -0.268104 0.000125 O 2.327999 -0.345489 0.021953 O -0.250828 -1.724508 -0.024825 C -3.209228 -0.439260 0.015263 H -3.407417 0.629260 -0.012777 H -2.639296 -0.724863 -0.867153 H -4.146196 -0.990611 0.030638 H -2.637614 -0.677663 0.910464 Cl -0.219101 1.611407 -0.007811	Cr -0.649187 -0.341628 -0.000000 O -2.142313 -0.698603 0.000160 O 0.631977 -1.566965 -0.000221 C 2.851958 -0.277137 0.000139 H 2.813869 0.323782 0.901848 H 1.860050 -0.937541 -0.000059 H 3.652441 -1.009909 0.001407 H 2.815221 0.322185 -0.902688 Cl -0.034716 1.722819 -0.000050	Cr 0.756050 -0.302480 -0.000000 O 2.282984 -0.477391 -0.000017 O -0.405771 -1.611108 0.000018 C -3.290567 -0.331661 -0.000015 H -3.008189 0.134099 -0.928733 H -1.370403 -1.490282 0.000029 H -3.957346 -1.176604 0.000069 H -3.008112 0.134218 0.928621 Cl -0.122085 1.668002 0.000006
4et i-type	Cr -0.199089 0.136133 0.005999 O 0.737292 -1.393501 0.017016 O 0.389143 1.550115 0.009138 C 3.502841 -0.110980 -0.015803 H 4.566465 0.115833 -0.012762 H 3.045972 0.333420 -0.897890 H 3.047177 0.305382 0.880542 H 3.362255 -1.189203 -0.032673 Cl -2.310134 -0.201156 -0.011507	Cr -0.172711 0.183032 0.000704 O 0.950298 -1.176925 0.002775 O 0.243734 1.663273 0.000797 C 3.315100 -0.203909 -0.002385 H 3.814596 -0.562314 0.891164 H 3.791221 -0.532326 -0.919833 H 3.118368 0.862453 0.017573 H 2.253525 -0.750384 0.003454 Cl -2.251501 -0.357501 -0.001384	Cr 0.339373 0.303562 -0.000239 O -1.094036 -0.686335 -0.000656 O 0.410842 1.838834 0.000262 C -4.235199 -0.337019 0.000174 H -4.290312 -0.909512 -0.909587 H -4.302034 -0.836694 0.951079 H -4.245734 0.738241 -0.041910 H -2.055434 -0.555182 0.001712 Cl 2.213253 -0.760012 0.000386
2et p-type	Cr -0.361939 -0.283431 0.000009 O -0.926944 -0.858546 1.336594 O -0.926777 -0.857115 -1.337271 C -0.676079 2.099083 0.000495 H -0.629653 1.536911 -0.947763 H -1.629110 2.617951 0.001280 H 0.172457 2.774080 -0.000007 H -0.628283 1.536753 0.948620 Cl 1.781609 -0.031327 0.000006	Cr -0.240719 -0.317245 0.073642 O -1.077132 0.018382 1.442800 O -0.702036 -1.425373 -0.898277 C -1.083531 1.489857 -0.705547 H -0.866839 1.095453 -1.696719 H -2.141974 1.747546 -0.684443 H -0.446118 2.342164 -0.496158 H -1.283357 0.954512 0.559424 Cl 1.838240 0.223000 0.025153	Cr -0.286032 -0.111535 -0.204464 O -1.209289 -1.374973 0.552018 O -0.759211 0.436117 -1.552904 C -0.759223 1.413579 0.977546 H -0.212418 2.282300 0.625017 H -1.835311 1.550980 0.926895 H -0.426269 1.116360 1.970391 H -1.395405 -1.474459 1.492300 Cl 1.825736 -0.104057 0.119667
2et p-type	Cr -0.361853 -0.283416 -0.000017 O -0.926822 -0.857829 -1.336919 O -0.926105 -0.858343 1.336987 C -0.677035 2.098498 0.000264 H 0.170501 2.774778 0.002300 H -1.630746 2.616071 -0.001624 H -0.630766 1.535991 0.948375 H -0.626722 1.536474 -0.947877 Cl 1.781636 -0.030762 -0.000170	Cr 0.271333 0.457029 -0.090734 O 0.549461 1.861856 0.492115 O -1.193692 0.171380 -0.937839 C -3.038134 -0.795555 0.463230 H -3.751128 -1.180598 -0.255990 H -2.131203 -0.291547 -0.313021 H -2.526864 -1.558476 1.037776 H -3.391756 0.047781 1.043180 Cl 1.686566 -1.145789 0.085416	Cr 0.338103 0.301524 -0.000399 O 0.404186 1.837078 0.000385 O -1.090423 -0.695198 -0.001710 C -4.235834 -0.332738 0.000658 H -4.293392 -0.916257 -0.902001 H -2.052435 -0.569710 0.002277 H -4.312821 -0.819006 0.957743 H -4.235002 0.741989 -0.055644 Cl 2.216710 -0.753659 0.000816
2et p-type	Cr 0.361577 -0.283571 -0.000030	Cr 0.302524 0.446636 0.108863	Cr 0.348256 0.312566 0.000118

	O 0.927055 -0.858676 -1.336436 O 0.925013 -0.858145 1.337445 C 0.678607 2.097642 0.000052 H 0.630017 1.536172 -0.948504 H -0.168610 2.774280 0.000933 H 1.632527 2.614890 -0.000136 H 0.631039 1.534835 0.947982 Cl -1.781823 -0.029750 -0.000467	O 0.567594 1.845818 -0.478378 O -1.200501 0.175913 0.827909 C -3.173007 -0.769134 -0.418678 H -2.735633 -1.643963 -0.881626 H -2.143426 -0.248050 0.303886 H -3.894003 -0.968031 0.363747 H -3.424800 0.040270 -1.091189 Cl 1.708152 -1.144619 -0.093630	O 0.455640 1.845685 -0.000113 O -1.107519 -0.643931 0.000695 C -4.260099 -0.352319 -0.000323 H -4.337271 0.104019 -0.971816 H -2.067133 -0.501654 -0.000178 H -4.217594 -1.424653 0.085184 H -4.354327 0.252606 0.884540 Cl 2.199635 -0.790118 -0.000193